Journal of Sound and Vibration 329 (2010) 1853–1874

Contents lists available at ScienceDirect

Journal of Sound and Vibration

journal homepage: www.elsevier.com/locate/jsvi

Nonlinear nonuniform torsional vibrations of bars by the boundary element method

E.J. Sapountzakis *, V.J. Tsipiras

Institute of Structural Analysis, School of Civil Engineering, National Technical University of Athens, Zografou Campus, GR – 157 80 Athens, Greece

ARTICLE INFO

Article history:
Received 17 February 2009
Received in revised form
20 November 2009
Accepted 26 November 2009
Handling Editor: M.P. Cartmell
Available online 22 December 2009

ABSTRACT

In this paper a boundary element method is developed for the nonuniform torsional vibration problem of bars of arbitrary doubly symmetric constant cross-section taking into account the effect of geometrical nonlinearity. The bar is subjected to arbitrarily distributed or concentrated conservative dynamic twisting and warping moments along its length, while its edges are supported by the most general torsional boundary conditions. The transverse displacement components are expressed so as to be valid for large twisting rotations (finite displacement–small strain theory), thus the arising governing differential equations and boundary conditions are in general nonlinear. The resulting coupling effect between twisting and axial displacement components is considered and torsional vibration analysis is performed in both the torsional pre- or post-buckled state. A distributed mass model system is employed, taking into account the warping, rotatory and axial inertia, leading to the formulation of a coupled nonlinear initial boundary value problem with respect to the variable along the bar angle of twist and to an "average" axial displacement of the cross-section of the bar. The numerical solution of the aforementioned initial boundary value problem is performed using the analog equation method, a BEM based method, leading to a system of nonlinear differential-algebraic equations (DAE), which is solved using an efficient time discretization scheme. Additionally, for the free vibrations case, a nonlinear generalized eigenvalue problem is formulated with respect to the fundamental mode shape at the points of reversal of motion after ignoring the axial inertia to verify the accuracy of the proposed method. The problem is solved using the direct iteration technique (DIT), with a geometrically linear fundamental mode shape as a starting vector. The validity of negligible axial inertia assumption is examined for the problem at hand.

1. Introduction

When arbitrary torsional boundary conditions are applied either at the edges or at any other interior point of the bar due to construction requirements, this bar under the action of general twisting loading is leaded to nonuniform torsion. Besides, since weight saving is of paramount importance, frequently used thin-walled open sections have low torsional stiffness and their torsional deformations can be of such magnitudes that it is not adequate to treat the angles of cross-section rotation as small. In these cases, the study of nonlinear effects on these members becomes essential, where this nonlinearity results from retaining the nonlinear terms in the strain–displacement relations (finite displacement–small

* Corresponding author. Tel.: +30210 7721718; fax: +30210 7721720.
E-mail addresses: cvsapoun@central.ntua.gr (E.J. Sapountzakis), tsipiras@gmail.com (V.J. Tsipiras).

0022-460X/$ - see front matter © 2009 Elsevier Ltd. All rights reserved.
doi:10.1016/j.jsv.2009.11.035

strain theory). When finite twist rotation angles are considered, the nonuniform torsional dynamic analysis of bars becomes much more complicated, leading to the formulation of coupled and nonlinear torsional and axial equilibrium equations. In this case, accounting for the axial loading and boundary conditions becomes essential to perform a rigorous dynamic analysis of the bar.

When the twist rotation angles of a member are small, a wide range of linear analysis tools, such as modal analysis, can be used and some analytical results are possible. As these rotation angles become larger, the induced geometric nonlinearities result in effects that are not observed in linear systems. In such situations the possibility of an analytical solution method is significantly reduced and is restricted to special cases of bar boundary conditions or loading.

During the past few years, the nonlinear nonuniform torsional dynamic analysis of bars undergoing moderate large rotations has received a good amount of attention in the literature. More specifically, Rozmarynowski and Szymczak in [1] studied the nonlinear free torsional vibrations of axially immovable thin-walled beams with doubly symmetric open cross-section, employing the finite element method. In this research effort only free vibrations are examined, the solution is provided only at points of reversal of motion (not in the time domain), no general axial, torsional or warping boundary conditions (elastic support case) are studied, while some nonlinear terms related to the finite twisting rotations as well as the axial inertia term are ignored. Crespo Da Silva in [2–3] presented the nonlinear flexural–torsional–extensional vibrations of Euler–Bernoulli doubly symmetric thin-walled closed cross-section beams, primarily focusing to flexural vibrations and neglecting the effect of torsional warping. Pai and Nayfeh in [4–6] studied also the nonlinear flexural–torsional–extensional vibrations of metallic and composite slewing or rotating closed cross-section beams, primarily focusing to flexural vibrations and neglecting again the effect of torsional warping. Di Egidio et al. in [7–8] presented also a FEM solution to the nonlinear flexural–torsional vibrations of shear undeformable thin-walled open beams taking into account in-plane and out-of-plane warpings and neglecting warping inertia. In these papers, the torsional–extensional coupling is taken into account but the inextensionality assumption leads to the fact that the axial boundary conditions are not general. Simo and Vu-Quoc in [9] presented a FEM solution to a fully nonlinear (small or large strains, hyperelastic material) three dimensional rod model including the effects of transverse shear and torsion-warping deformation based on a geometrically exact description of the kinematics of deformation. Moreover, Pai and Nayfeh in [10] studied a geometrically exact nonlinear curved beam model for solid composite rotor blades using the concept of local engineering stress and strain measures and taking into account the in-plane and out-of-plane warpings. In the last two research efforts, the out-of-plane buckling of a framed structure and a helical spring have been analyzed, respectively, thus the extensional–torsional coupling is not discussed. Mohri et al. in [11] proposed a FEM solution to the linear vibration analysis of pre- and post-buckled thin-walled open cross-section beams, neglecting warping and axial inertia, considering geometrical nonlinearity only for the static loading and presenting examples of bars subjected to free vibrations and special boundary conditions. Finally, Machado and Cortinez in [12] presented also a FEM solution to the linear free vibration analysis of bisymmetric thin-walled composite beams with open cross-section, taking into account static initial stresses and deformations considering geometrical nonlinearity only for the static loading and presenting examples of bars subjected to special boundary conditions. The boundary element method has not yet been used for the nonlinear nonuniform torsional dynamic analysis of bars.

In this paper a boundary element method is developed for the nonuniform torsional vibration problem of bars of arbitrary doubly symmetric constant cross-section taking into account the effect of geometrical nonlinearity (finite displacement–small strain theory). A coupled nonlinear initial boundary value problem with respect to the variable along the bar angle of twist and to an ‘‘average’’ axial displacement of the cross-section of the bar is formulated and numerically solved using the analog equation method [13], a BEM based method, leading to a system of nonlinear differential-algebraic equations (DAE). Additionally, for the free vibrations case, a nonlinear generalized eigenvalue problem is formulated with respect to the fundamental mode shape at the points of reversal of motion (after ignoring the axial inertia) to verify the accuracy of the proposed method. The problem is solved using the direct iteration technique (DIT) [14]. The main objective of the present contribution is to focus on the torsional–extensional coupling of bars and provide the corresponding governing differential equations without dropping any nonlinear or inertial terms. Moreover, the influence of the axial inertia term on the response of the bar under nonlinear torsional vibrations is investigated, while numerical examples of both free and forced vibrations are presented. The essential features and novel aspects of the present formulation compared with previous ones are summarized as follows:

(i) The cross-section is an arbitrarily shaped doubly symmetric thin or thick walled one. The formulation does not stand on the assumption of a thin-walled structure and therefore the cross-section’s torsional and warping rigidities are evaluated ‘‘exactly’’ in a numerical sense after formulating a boundary value problem with respect to the primary warping function.

(ii) The beam is supported by the most general boundary conditions including elastic support or restraint while a distributed mass model system is employed, taking into account all the inertial terms (warping, rotatory and axial inertia).

(iii) Previous research efforts except for [1] have not focused in the investigation of nonlinear torsional vibrations and the arising torsional–extensional coupling, while the improvements of the proposed method come up considering reference [1] where (a) the solution is provided only at points of reversal of motion—not in the time domain, (b) the

torsional, warping and axial boundary conditions do not include the elastic support case, (c) some nonlinear terms related to finite twisting rotations as well as the axial inertia term are not included in the analysis, and (d) forced vibrations are not considered.

(iv) The proposed method employs a BEM approach (requiring boundary discretization for the cross-sectional analysis) resulting in line or parabolic elements instead of area elements of the FEM solutions (requiring the whole cross-section to be discretized into triangular or quadrilateral area elements), while a small number of line elements are required to achieve high accuracy.

Numerical examples are worked out to investigate the effects of the nonlinear torsional vibrations such as the coupling between the torsional and axial equilibrium equations and the axial inertia terms.

2. Statement of the problem

2.1. Displacements, strains, stresses

Let us consider a prismatic beam of length l (Fig. 1), of constant arbitrary doubly symmetric cross-section of area A. The homogeneous isotropic and linearly elastic material of the beam cross-section, with modulus of elasticity E, shear modulus G and mass density ρ occupies the two dimensional multiply connected region Ω of the y, z plane and is bounded by the Γ_j $(j=1,2,\ldots,K)$ boundary curves, which are piecewise smooth, i.e. they may have a finite number of corners. In Fig. 1b *Syz* is the principal bending coordinate system through the cross-section's shear center. The bar is subjected to the combined action of the arbitrarily distributed or concentrated time dependent conservative axial load $n(x,t)$, twisting $m_t = m_t(x,t)$ and warping $m_w = m_w(x,t)$ moments acting in the x direction (Fig. 1a).

Under the aforementioned loading, the displacement field of the bar for large twisting rotations is given as

$$u(x,y,z,t) = u_m(x,t) + \theta_x'(x,t)\cdot\phi_S^P(y,z) \tag{1a}$$

$$v(x,y,z,t) = -z\cdot\sin\theta_x(x,t) - y(1-\cos\theta_x(x,t)) \tag{1b}$$

$$w(x,y,z,t) = y\cdot\sin\theta_x(x,t) - z(1-\cos\theta_x(x,t)) \tag{1c}$$

where u, v, w are the axial and transverse bar displacement components with respect to the *Syz* system of axes [15]; $\theta_x'(x,t)$ denotes the rate of change of the angle of twist $\theta_x(x,t)$ regarded as the torsional curvature; ϕ_S^P is the primary warping function with respect to the shear center S, respectively [16], and $u_m(x,t)$ is an "average" axial displacement of the cross-section of the bar, that will be later explained.

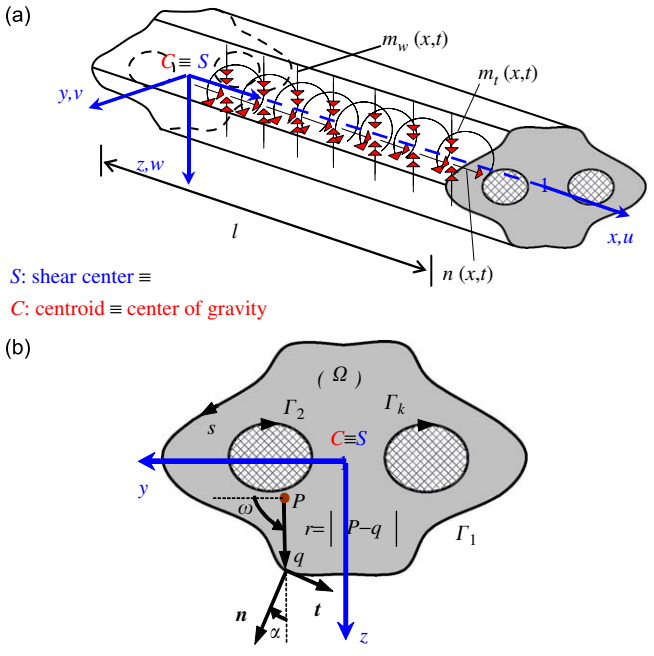

Fig. 1. Prismatic element subjected to axial and torsional loading (a) with an arbitrarily shaped doubly symmetric constant cross-section occupying the region Ω (b).

Employing the strain–displacement relations of the three dimensional elasticity for moderate displacements, the following strain components can be easily obtained :

$$\varepsilon_{xx}=\frac{\partial u}{\partial x}+\frac{1}{2}\left[\left(\frac{\partial v}{\partial x}\right)^2+\left(\frac{\partial w}{\partial x}\right)^2\right] \tag{2a}$$

$$\gamma_{xy}=\frac{\partial u}{\partial y}+\frac{\partial v}{\partial x}+\frac{\partial v}{\partial y}\frac{\partial v}{\partial x}+\frac{\partial w}{\partial y}\frac{\partial w}{\partial x} \tag{2b}$$

$$\gamma_{xz}=\frac{\partial w}{\partial x}+\frac{\partial u}{\partial z}+\frac{\partial v}{\partial z}\frac{\partial v}{\partial x}+\frac{\partial w}{\partial z}\frac{\partial w}{\partial x} \tag{2c}$$

where it has been assumed that for moderate displacements $(\partial u/\partial x)^2 \ll \partial u/\partial x$, $(\partial u/\partial x)(\partial u/\partial y) \ll (\partial v/\partial x)+(\partial u/\partial y)$, $(\partial u/\partial x)(\partial u/\partial z) \ll (\partial w/\partial x)+(\partial u/\partial z)$ [17,18,19]. Substituting the displacement components (1) to the strain–displacement relations (2), the nonvanishing strain resultants are obtained as

$$\varepsilon_{xx}=u'_m+\theta''_x\cdot\phi_S^P(y,z)+\tfrac{1}{2}(y^2+z^2)(\theta'_x)^2 \tag{3a}$$

$$\gamma_{xy}=\theta'_x\left(\frac{\partial\phi_S^P}{\partial y}-z\right) \tag{3b}$$

$$\gamma_{xz}=\theta'_x\left(\frac{\partial\phi_S^P}{\partial z}+y\right) \tag{3c}$$

where the second-order geometrically nonlinear term in the right hand side of Eq. (3a) $(y^2+z^2)(\theta'_x)^2/2$ is often described as the "Wagner strain" [20].

Considering strains to be small and employing the second Piola–Kirchhoff stress tensor, the work contributing stress components are defined in terms of the strain ones as

$$\begin{Bmatrix} S_{xx}\\ S_{xy}\\ S_{xz}\end{Bmatrix}=\begin{bmatrix} E^* & 0 & 0\\ 0 & G & 0\\ 0 & 0 & G\end{bmatrix}\begin{Bmatrix}\varepsilon_{xx}\\ \gamma_{xy}\\ \gamma_{xz}\end{Bmatrix} \tag{4}$$

where E^* is obtained from Hooke's stress–strain law as $E^*=E(1-\nu)/(1+\nu)(1-2\nu)$. If the plane stress hypothesis is undertaken then $E^*=E/1\text{-}\nu^2$ holds [21], while E is frequently considered instead of E^* ($E^*\approx E$) in beam formulations [21,22]. This last consideration has been followed throughout the paper, although it is stressed out that any other reasonable expression of E^* could also be used without any difficulty.

2.2. Evaluation of the primary warping function ϕ_S^P

The primary warping function is evaluated independently from the following boundary value problem [16,23]:

$$\nabla^2\phi_S^P=0 \quad \text{in } \Omega \tag{5a}$$

$$\frac{\partial\phi_S^P}{\partial n}=z\cdot n_y-y\cdot n_z \quad \text{on } \Gamma_j \tag{5b}$$

where $\nabla^2=\partial^2/\partial y^2+\partial^2/\partial z^2$ is the Laplace operator and $\partial/\partial n$ denotes the directional derivative normal to the boundary Γ. Since the problem at hand has Neumann type boundary condition, the evaluated warping function contains an integration constant (parallel displacement of the cross-section along the bar axis), which is evaluated by inducing the following constraint:

$$\int_\Omega\phi_S^P\,\mathrm{d}\Omega=0 \tag{6}$$

It is worth pointing out that any other constraint could be used, although the use of Eq. (6) decouples the governing equations of the torsional problem at the greatest extent. Based on Eq. (6), the meaning of the "average" axial displacement of the cross-section of the bar can now be explained as Eq. (1a) can be written as

$$\int_\Omega u\,\mathrm{d}\Omega=u_m\cdot A+\theta'_x\cdot\int_\Omega\phi_S^P\,\mathrm{d}\Omega \tag{7}$$

which leads to the relation

$$u_m=\frac{\int_\Omega u\,\mathrm{d}\Omega}{A} \tag{8}$$

2.3. Equations of global equilibrium

The stress resultants of the bar are defined as

$$N = \int_{\Omega} S_{xx}\, d\Omega \tag{9a}$$

$$M_t^P = \int_{\Omega} \left[S_{xy}^P \left(\frac{\partial \phi_S^P}{\partial y} - z \right) + S_{xz}^P \left(\frac{\partial \phi_S^P}{\partial z} + y \right) \right] d\Omega \tag{9b}$$

$$M_w = -\int_{\Omega} S_{xx} \phi_S^P\, d\Omega \tag{9c}$$

where M_t^P is the primary twisting moment [16] resulting from the primary shear stress distribution ($S_{xy}^P = S_{xy}$, $S_{xz}^P = S_{xz}$ hold since warping shear stresses are not taken into account within the present formulation) and M_w is the warping moment (bimoment) due to the torsional curvature [16,21]. It is noted that Eq. (9b) could also be written as

$$M_t^P = \int_{\Omega} [S_{xy}^P(-z) + S_{xz}^P y]\, d\Omega$$

by substituting the expressions of shear stresses, carrying out suitable integrations by parts and finally exploiting Eq. (5). Substituting Eq. (4) into Eq. (9) the stress resultants are obtained as

$$N = EA \left[u_m' + \frac{1}{2} \frac{I_P}{A} (\theta_x')^2 \right] \tag{10a}$$

$$M_t^P = GI_t \cdot \theta_x' \tag{10b}$$

$$M_w = -EC_S \cdot \theta_x'' \tag{10c}$$

where the polar moment of inertia I_P, the torsion constant I_t and the warping constant C_S with respect to the shear center S are given as

$$I_P = \int_{\Omega} (y^2 + z^2)\, d\Omega \tag{11a}$$

$$I_t = \int_{\Omega} \left(y^2 + z^2 + y \cdot \frac{\partial \phi_S^P}{\partial z} - z \cdot \frac{\partial \phi_S^P}{\partial y} \right) d\Omega \tag{11b}$$

$$C_S = \int_{\Omega} (\phi_S^P)^2\, d\Omega \tag{11c}$$

It is worth here noting that the aforementioned stress resultants refer to the directions of the cross-section at its deformed configuration (the cross-sections' rotations are taken into account), since they have been defined with respect to the second Piola–Kirchhoff stress tensor. Nevertheless, the expressions of the primary twisting and warping moments (Eq. (10b) and (10c)) are proven to be identical with those of the linear case [21].

The principle of virtual work under a total Lagrangian formulation

$$\delta W_{\text{int}} + \delta W_{\text{mass}} = \delta W_{\text{ext}} \tag{12}$$

where

$$\delta W_{\text{int}} = \int_V (S_{xx} \delta \varepsilon_{xx} + S_{xy} \delta \gamma_{xy} + S_{xz} \delta \gamma_{xz})\, dV \tag{13a}$$

$$\delta W_{\text{mass}} = \int_V \rho (\ddot{u} \delta u + \ddot{v} \delta v + \ddot{w} \delta w)\, dV \tag{13b}$$

$$\delta W_{\text{ext}} = \int_F (t_x \cdot \delta u + t_y \cdot \delta v + t_z \cdot \delta w)\, dF \tag{13c}$$

is employed to obtain global equilibrium equations. In the above equations, $\delta(\cdot)$ denotes virtual quantities, $(\cdot)$ denotes differentiation with respect to time, V, F are the volume and the surface of the bar, respectively, at the initial configuration and t_x, t_y, t_z are the components of the traction vector with respect to the undeformed surface of the bar. Substituting the stress resultants given in Eq. (4), the strain ones given in Eq. (3) and the displacement components given in Eqs. (1)–(12), the governing partial differential equations of the bar are obtained after some algebra as

$$\rho A \cdot \ddot{u}_m - \frac{\partial N}{\partial x} = n(x,t) \tag{14a}$$

$$\rho I_P \cdot \ddot{\theta}_x - \rho C_S \cdot \ddot{\theta}_x'' - \frac{\partial M_t^P}{\partial x} - \frac{\partial^2 M_w}{\partial x^2} - \frac{3}{2} E I_{PP} (\theta_x')^2 \theta_x'' - E I_P \cdot u_m' \, \theta_x'' - E I_P \cdot u_m'' \, \theta_x' = m_t(x,t) + \frac{\partial}{\partial x}[m_w(x,t)] \tag{14b}$$

while the corresponding boundary conditions at the bar ends are written as

$$(N - \overline{N}) \delta u_m = 0 \tag{15a}$$

$$[(M_w)' + M_t^P + \tfrac{1}{2} E I_{PP} (\theta_x')^3 + E I_P \cdot u_m' \, \theta_x' - \overline{M_t}] \delta\theta_x = 0 \tag{15b}$$

$$(-M_w + \overline{M_w}) \delta\theta_x' = 0 \tag{15c}$$

where the geometric cross-sectional property I_{PP} is given as

$$I_{PP} = \int_\Omega (y^2 + z^2)^2 \, \mathrm{d}\Omega \tag{16}$$

In Eq. (15), $\overline{N}, \overline{Mt}, \overline{M_w}$ are the externally applied conservative time dependent axial force, twisting and warping moments at the bar ends, respectively. The expressions of the externally applied loads with respect to the first Piola–Kirchhoff stress components can be easily deduced by virtue of Eq. (13c). It is worth here noting that in deriving the governing equations of the bar the secondary shear stress distribution has been ignored [24]. Employing Eq. (10), the governing partial differential equations of the initial boundary value problem of the bar are formulated as

$$\rho A \cdot \ddot{u}_m - E A \cdot u_m'' - E I_P \cdot \theta_x' \, \theta_x'' = n(x,t) \tag{17a}$$

$$\rho I_P \cdot \ddot{\theta}_x - \rho C_S \cdot \ddot{\theta}_x'' - G I_t \theta_x'' + E C_S \theta_x'''' - \frac{3}{2} E I_{PP} \cdot (\theta_x')^2 \theta_x'' - E I_P \cdot u_m' \, \theta_x'' - E I_P \cdot u_m'' \, \theta_x' = m_t(x,t) + \frac{\partial}{\partial x}[m_w(x,t)] \tag{17b}$$

subjected to the initial conditions ($x \in (0, l)$)

$$u_m(x,0) = \overline{u}_{m0}(x), \quad \dot{u}_m(x,0) = \dot{\overline{u}}_{m0}(x) \tag{18a,b}$$

$$\theta_x(x,0) = \overline{\theta}_{x0}(x), \quad \dot{\theta}_x(x,0) = \dot{\overline{\theta}}_{x0}(x) \tag{18c,d}$$

together with the boundary conditions at the bar ends $x = 0, l$

$$a_1 N + \alpha_2 u_m = \alpha_3 \tag{19a}$$

$$\beta_1 M_t + \beta_2 \theta_x = \beta_3, \quad \overline{\beta}_1 M_w + \overline{\beta}_2 \theta_x' = \overline{\beta}_3 \tag{19b,c}$$

where N, M_t, M_w are the axial force, twisting and warping moments at the bar ends, respectively, given as

$$N = E A \cdot u_m' + \tfrac{1}{2} E I_P (\theta_x')^2 \tag{20a}$$

$$M_t = G I_t \theta_x' - E C_S \theta_x''' + E I_P \cdot u_m' \, \theta_x' + \tfrac{1}{2} E I_{PP} (\theta_x')^3 \tag{20b}$$

$$M_w = -E C_S \cdot \theta_x'' \tag{20c}$$

while $a_i, \beta_i, \overline{\beta}_i$ ($i = 1, 2, 3$) are time dependent functions specified at the boundary of the bar. The boundary conditions (19) are the most general boundary conditions for the problem at hand, including also the elastic support. It is apparent that all types of the conventional torsional boundary conditions (clamped, simply supported, free or guided edge) can be derived from Eq. (19b,c) by specifying appropriately the functions β_i and $\overline{\beta}_i$ (e.g. for a clamped edge it is $\beta_2 = \overline{\beta}_2 = 1$, $\beta_1 = \beta_3 = \overline{\beta}_1 = \overline{\beta}_3 = 0$, for a simply supported edge $\beta_2 = \overline{\beta}_1 = 1$, $\beta_1 = \beta_3 = \overline{\beta}_2 = \overline{\beta}_3 = 0$ and for a free edge $\beta_1 = \overline{\beta}_1 = 1$, $\beta_2 = \beta_3 = \overline{\beta}_2 = \overline{\beta}_3 = 0$). It is worth here noting that at clamped edges warping is fully restrained (i.e. the longitudinal displacement $u = 0$), therefore the term $\theta_x' \cdot \phi_S^P$ of Eq. (1a) must vanish. This condition is mathematically accomplished if θ_x' equals to zero which is the exact expression ($\theta_x' = 0$) of the warping boundary condition for the clamped edge [16]. The terms of the boundary conditions of Eq. (19) are nonlinear by virtue of Eq. (20), while damping could also be included in Eq. (17) without any special difficulty.

The solution of the initial boundary value problem described by Eqs. (17)–(19), for the evaluation of the unknown displacement components assumes that the warping C_S and the torsion I_t constants defined from Eq. (11b,c) are already established. Eq. (11b,c) indicate that the evaluation of the aforementioned constants presumes that the primary warping function ϕ_S^P at any interior point of the domain Ω of the cross-section of the bar is evaluated after solving the boundary value problem described by Eq. (5a,b). Once $u_m(x,t)$, $\theta_x(x,t)$ are established, the stress components and the displacement field can be evaluated employing Eqs. (4) and (1), respectively.

The established initial boundary value problem is strongly coupled and nonlinear. A significant reduction on the set of differential equations can be achieved by neglecting the axial inertia term $\rho A \cdot \ddot{u}_m$ of Eq. (17a), a common assumption among dynamic beam formulations. Ignoring this term a single partial differential equation along with a single unknown displacement component (the angle of twist $\theta_x(x,t)$) is obtained, which is further simplified in the case of vanishing distributed axial load along the bar. In what follows, this procedure is described in detail for the cases of axially immovable ends and constant axial load along the bar which are of great practical interest, while the aforementioned term will be

taken into account in the section of numerical analysis for the first time in the literature for the nonlinear nonuniform torsional vibrations problem investigating the influence of its ignorance.

2.4. Reduced initial boundary value problem for special cases of axial boundary conditions

For the case of axially immovable ends, the axial boundary conditions (19a) are written as

$$u_m(0,t)=0, \quad u_m(l,t)=0 \tag{21a,b}$$

Employing the aforementioned simplifications, Eq. (17a) gives

$$u''_m = -\frac{I_P}{A}\cdot\theta'_x\,\theta''_x\,, \quad \forall x\in(0,l) \tag{22}$$

which after subsequent integration and utilization of Eq. (21) yields

$$u'_m = -\frac{1}{2}\frac{I_P}{A}(\theta'_x)^2+\frac{\tilde{N}}{EA}, \quad \forall x\in[0,l] \tag{23}$$

where $\tilde{N}$ is a time-dependent tensile axial load induced by the geometrical nonlinearity given as

$$\tilde{N}=\frac{1}{2}\frac{EI_P}{l}\cdot\int_0^l(\theta'_x)^2\,\mathrm{d}x \tag{24}$$

For the case of constant along the bar axial load Eq. (22) holds, while the axial boundary conditions (19a) are written as

$$u_m(0,t)=0, N(l,t)=\overline{N}(l,t) \tag{25a,b}$$

In this case, Eq. (23) holds by setting $\tilde{N}=\overline{N}(l,t)$.

Substituting Eqs. (22), (23) into Eqs. (17b), (20b) the reduced initial boundary value problem is established as

$$\rho I_P\cdot\ddot{\theta}_x-\rho C_S\cdot\ddot{\theta}''_x-\left(GI_t+\frac{I_P}{A}\tilde{N}\right)\theta''_x+EC_S\theta''''_x-\frac{3}{2}EI_n(\theta'_x)^2\theta''_x=m_t(x,t)+\frac{\partial}{\partial x}[m_w(x,t)] \tag{26}$$

along with the pertinent initial conditions (18c,d) and the boundary conditions (19b,c). It is worth here noting that Eqs. (20a,c) hold, whereas Eq. (20b) is modified as

$$M_t=\left(GI_t+\frac{I_P}{A}\tilde{N}\right)\theta'_x-EC_S\cdot\theta'''_x+\frac{1}{2}EI_n(\theta'_x)^3 \tag{27}$$

In Eqs. (26) and (27) I_n is a nonnegative geometric cross-sectional property, related to the geometrical nonlinearity, defined as

$$I_n=I_{PP}-\frac{I_P^2}{A} \tag{28}$$

Comparing Eqs. (26), (27), (20a,c) with the corresponding set presented by Rozmarynowski and Szymczak in [1], the following improvements are noted:

- In Ref. [1], the torsional and warping boundary conditions do not include the elastic support case.
- In Ref. [1], both the partial differential equation and the torsional boundary condition do not include the nonlinear terms related to the finite twisting rotation. The influence of the ignorance of these terms will be subsequently numerically investigated.

3. Integral representations—numerical solution

3.1. For the axial displacement u_m and the angle of twist θ_x

According to the precedent analysis, the nonlinear nonuniform torsional vibration problem of a bar reduces in establishing the displacement components $u_m(x,t)$ and $\theta_x(x,t)$ having continuous partial derivatives up to the second and fourth order with respect to x, respectively, and up to the second order with respect to t, satisfying the nonlinear initial boundary value problem described by the coupled governing Eq. (17) along the bar, the initial conditions (18) and the boundary conditions (19) at the bar ends $x=0,l$.

Eqs. (17)–(19) are solved using the analog equation method [13] as it is developed for hyperbolic differential equations [25]. According to this method, let $u_m(x,t)$ and $\theta_x(x,t)$ be the sought solutions of the aforementioned problem. Setting as $u_1(x,t)=u_m(x,t)$, $u_2(x,t)=\theta_x(x,t)$ and differentiating with respect to x these functions two and four times, respectively, yields

$$\frac{\partial^2 u_1}{\partial x^2}=q_1(x,t), \quad \frac{\partial^4 u_2}{\partial x^4}=q_2(x,t) \tag{29a,b}$$

Eqs. (29) are quasi-static, that is the time variable appears as a parameter. They indicate that the solution of Eqs. (17)–(19) can be established by solving Eq. (29) under the same boundary conditions (19), provided that the fictitious load distributions $q_i(x,t)$ $(i=1,2)$ are first established. These distributions can be determined using BEM as follows.

The solutions of Eq. (29a,b) are given in integral form as [25]

$$u_1(x,t)=\int_0^l q_1 u_1^*\,\mathrm{d}\xi-\left[u_1^*\frac{\partial u_1}{\partial x}-\frac{\mathrm{d}u_1^*}{\mathrm{d}x}u_1\right]_{x=0}^{x=l} \tag{30a}$$

$$u_2(x,t)=\int_0^l q_2 u_2^*\,\mathrm{d}\xi-\left[u_2^*\frac{\partial^3 u_2}{\partial x^3}-\frac{\mathrm{d}u_2^*}{\mathrm{d}x}\frac{\partial^2 u_2}{\partial x^2}+\frac{\mathrm{d}^2u_2^*}{\mathrm{d}x^2}\frac{\partial u_2}{\partial x}-\frac{\mathrm{d}^3u_2^*}{\mathrm{d}x^3}u_2\right]_0^l \tag{30b}$$

where u_1^*, u_2^* are the fundamental solutions given as

$$u_1^*=\frac{1}{2}|r|,\quad u_2^*=\frac{1}{12}l^3\left(2+\left|\frac{r}{l}\right|^3-3\left|\frac{r}{l}\right|^2\right) \tag{31a,b}$$

with $r=x\text{-}\xi$, x,ξ points of the bar, which are particular singular solutions of the equations

$$\frac{\mathrm{d}^2u_1^*}{\mathrm{d}x^2}=\delta(x-\xi),\frac{\mathrm{d}^4u_2^*}{\mathrm{d}x^4}=\delta(x-\xi) \tag{32a,b}$$

Employing Eqs. (31a,b), the integral representations (30a,b) can be written as

$$u_1(x,t)=\int_0^l q_1\left(\Lambda_2(r)+\frac{1}{2}l\right)\mathrm{d}\xi-\left[\left(\Lambda_2(r)+\frac{1}{2}l\right)\frac{\partial u_1}{\partial x}+\Lambda_1(r)u_1\right]_0^l \tag{33a}$$

$$u_2(x,t)=\int_0^l q_2\Lambda_4(r)\,\mathrm{d}\xi-\left[\Lambda_4(r)\frac{\partial^3u_2}{\partial x^3}+\Lambda_3(r)\frac{\partial^2u_2}{\partial x^2}+\Lambda_2(r)\frac{\partial u_2}{\partial x}+\Lambda_1(r)u_2\right]_0^l \tag{33b}$$

where the kernels $\Lambda_j(r)$, $(j=1,2,3,4)$ are given in Appendix A. Notice that in Eqs. (33a,b), for the line integrals it is $r=x\text{-}\xi$, x, ξ points inside the bar, whereas for the rest terms it is $r=x\text{-}\zeta$, x inside the bar, ζ at the bar ends 0,l.

Differentiating Eqs. (33a,b) with respect to x, results in the integral representations of the derivatives of u_i as

$$\frac{\partial u_1(x,t)}{\partial x}=\int_0^l q_1\Lambda_1(r)\,\mathrm{d}\xi-\left[\Lambda_1(r)\frac{\partial u_1}{\partial x}\right]_{x=0}^{x=l} \tag{34a}$$

$$\frac{\partial^2u_1(x,t)}{\partial x^2}=q_1(x,t) \tag{34b}$$

$$\frac{\partial u_2(x,t)}{\partial x}=\int_0^l q_2\Lambda_3(r)\,\mathrm{d}\xi-\left[\Lambda_3(r)\frac{\partial^3u_2}{\partial x^3}+\Lambda_2(r)\frac{\partial^2u_2}{\partial x^2}+\Lambda_1(r)\frac{\partial u_2}{\partial x}\right]_0^l \tag{34c}$$

$$\frac{\partial^2u_2(x,t)}{\partial x^2}=\int_0^l q_2\Lambda_2(r)\,\mathrm{d}\xi-\left[\Lambda_2(r)\frac{\partial^3u_2}{\partial x^3}+\Lambda_1(r)\frac{\partial^2u_2}{\partial x^2}\right]_0^l \tag{34d}$$

$$\frac{\partial^3u_2(x,t)}{\partial x^3}=\int_0^l q_2\Lambda_1(r)\,\mathrm{d}\xi-\left[\Lambda_1(r)\frac{\partial^3u_2}{\partial x^3}\right]_0^l \tag{34e}$$

$$\frac{\partial^4u_2(x,t)}{\partial x^4}=q_2(x,t) \tag{34f}$$

The integral representations (33a,b) and (34c) when applied to the bar ends $(0,l)$, together with the boundary conditions (19), are employed to express the unknown boundary quantities $u_i(\zeta,t)$, $u_{i,x}(\zeta,t)$, $u_{2,xx}(\zeta,t)$ and $u_{2,xxx}(\zeta,t)$ $(\zeta=0)$ in terms of q_i. This is accomplished numerically as follows.

The interval $(0,l)$ is divided into L elements (Fig. 2), on which $q_i(x,t)$ is assumed to vary according to certain law (constant, linear, parabolic, etc.). The constant element assumption is employed here as the numerical implementation becomes very simple and the obtained results are very good.

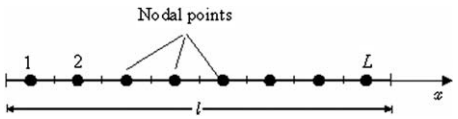

Fig. 2. Discretization of the beam interval and distribution of the nodal points.

Employing the aforementioned procedure, the following set of 12 nonlinear algebraic equations is obtained

$$\begin{bmatrix} \mathbf{F}_1 & \mathbf{E}_{12} & \mathbf{E}_{13} & \mathbf{0} & \mathbf{0} & \mathbf{0} & \mathbf{0} & \mathbf{0} \\ \mathbf{0} & \mathbf{D}_{22} & \mathbf{D}_{23} & \mathbf{0} & \mathbf{0} & \mathbf{0} & \mathbf{0} & \mathbf{0} \\ \mathbf{0} & \mathbf{0} & \mathbf{0} & \mathbf{F}_3 & \mathbf{E}_{35} & \mathbf{E}_{36} & \mathbf{E}_{37} & \mathbf{E}_{38} \\ \mathbf{0} & \mathbf{0} & \mathbf{0} & \mathbf{F}_4 & \mathbf{0} & \mathbf{E}_{46} & \mathbf{E}_{47} & \mathbf{E}_{48} \\ \mathbf{0} & \mathbf{0} & \mathbf{0} & \mathbf{0} & \mathbf{D}_{55} & \mathbf{D}_{56} & \mathbf{0} & \mathbf{D}_{58} \\ \mathbf{0} & \mathbf{0} & \mathbf{0} & \mathbf{0} & \mathbf{0} & \mathbf{D}_{66} & \mathbf{D}_{67} & \mathbf{0} \end{bmatrix} \begin{Bmatrix} \mathbf{q}_1 \\ \hat{\mathbf{u}}_1 \\ \hat{\mathbf{u}}_{1,x} \\ \mathbf{q}_2 \\ \hat{\mathbf{u}}_2 \\ \hat{\mathbf{u}}_{2,x} \\ \hat{\mathbf{u}}_{2,xx} \\ \hat{\mathbf{u}}_{2,xxx} \end{Bmatrix} + \begin{bmatrix} \mathbf{0} & \mathbf{0} & \mathbf{0} \\ \mathbf{D}_{21}^{\mathrm{nl}} & \mathbf{0} & \mathbf{0} \\ \mathbf{0} & \mathbf{0} & \mathbf{0} \\ \mathbf{0} & \mathbf{0} & \mathbf{0} \\ \mathbf{0} & \mathbf{D}_{52}^{\mathrm{nl}} & \mathbf{D}_{53}^{\mathrm{nl}} \\ \mathbf{0} & \mathbf{0} & \mathbf{0} \end{bmatrix} \begin{Bmatrix} \hat{\mathbf{u}}_2^2 \\ \hat{\mathbf{u}}_2^3 \\ \hat{\mathbf{u}}_1\hat{\mathbf{u}}_2 \end{Bmatrix} = \begin{Bmatrix} \mathbf{0} \\ \boldsymbol{\alpha}_3 \\ \mathbf{0} \\ \mathbf{0} \\ \boldsymbol{\beta}_3 \\ \overline{\boldsymbol{\beta}}_3 \end{Bmatrix} \tag{35}$$

where $\mathbf{D}_{22}$, $\mathbf{D}_{23}$, $\mathbf{D}_{55}$, $\mathbf{D}_{56}$, $\mathbf{D}_{58}$, $\mathbf{D}_{66}$, $\mathbf{D}_{67}$, $\mathbf{D}_{21}^{\mathrm{nl}}$, $\mathbf{D}_{52}^{\mathrm{nl}}$, $\mathbf{D}_{53}^{\mathrm{nl}}$ are 2×2 rectangular known, in general time dependent, matrices including the values of the functions $a_j, \beta_j, \overline{\beta}_j$ $(j=1,2)$ of Eq. (19a); $\boldsymbol{\alpha}_3$, $\boldsymbol{\beta}_3$, $\overline{\boldsymbol{\beta}}_3$ are 2×1 known, in general time dependent, column matrices including the boundary values of the functions $a_3, \beta_3, \overline{\beta}_3$ of Eq. (19a,b,c); $\mathbf{E}_{12}$, $\mathbf{E}_{13}$, $\mathbf{E}_{35}$, $\mathbf{E}_{36}$, $\mathbf{E}_{37}$, $\mathbf{E}_{38}$, $\mathbf{E}_{46}$, $\mathbf{E}_{47}$, $\mathbf{E}_{48}$ are rectangular 2×2 known coefficient matrices resulting from the values of the kernels $\Lambda_j(r)$ $(j=1,2,3,4)$ at the bar ends and $\mathbf{F}_1, \mathbf{F}_3, \mathbf{F}_4$ are $2\times L$ rectangular known matrices originating from the integration of the kernels on the axis of the bar. Moreover

$$\hat{\mathbf{u}}_i = \{u_i(0,t)\ \ u_i(l,t)\}^{\mathrm{T}} \quad (i=1,2) \tag{36a}$$

$$\hat{\mathbf{u}}_{i,x} = \left\{ \frac{\partial u_i(0,t)}{\partial x} \quad \frac{\partial u_i(l,t)}{\partial x} \right\}^{\mathrm{T}} \quad (i=1,2) \tag{36b}$$

$$\hat{\mathbf{u}}_{2,xx} = \left\{ \frac{\partial^2 u_2(0,t)}{\partial x^2} \quad \frac{\partial^2 u_2(l,t)}{\partial x^2} \right\}^{\mathrm{T}} \tag{36c}$$

$$\hat{\mathbf{u}}_{2,xxx} = \left\{ \frac{\partial^3 u_2(0,t)}{\partial x^3} \quad \frac{\partial^3 u_2(l,t)}{\partial x^3} \right\}^{\mathrm{T}} \tag{36d}$$

$$\hat{\mathbf{u}}_2^2 = \left\{ \left[\frac{\partial u_2(0,t)}{\partial x}\right]^2 \quad \left[\frac{\partial u_2(l,t)}{\partial x}\right]^2 \right\}^{\mathrm{T}} \tag{36e}$$

$$\hat{\mathbf{u}}_2^3 = \left\{ \left[\frac{\partial u_2(0,t)}{\partial x}\right]^3 \quad \left[\frac{\partial u_2(l,t)}{\partial x}\right]^3 \right\}^{\mathrm{T}} \tag{36f}$$

$$\hat{\mathbf{u}}_1\hat{\mathbf{u}}_2 = \left\{ \frac{\partial u_1(0,t)}{\partial x}\cdot\frac{\partial u_2(0,t)}{\partial x} \quad \frac{\partial u_1(l,t)}{\partial x}\cdot\frac{\partial u_2(l,t)}{\partial x} \right\}^{\mathrm{T}} \tag{36g}$$

are vectors including the two unknown time dependent boundary values of the respective boundary quantities and $\mathbf{q}_i = \{q_1^i q_2^i \cdots q_L^i\}^{\mathrm{T}}$ $(i=1,2)$ are vectors including the L unknown time dependent nodal values of the fictitious loads.

Discretization of Eqs. (33), (34) and application to the L collocation nodal points yields

$$\mathbf{u}_1 = \mathbf{A}_1^0\mathbf{q}_1 + \mathbf{C}_0\hat{\mathbf{u}}_1 + \mathbf{C}_1\hat{\mathbf{u}}_{1,x}, \quad \mathbf{u}_{1,x} = \mathbf{A}_1^1\mathbf{q}_1 + \mathbf{C}_0\hat{\mathbf{u}}_{1,x}, \quad \mathbf{u}_{1,xx} = \mathbf{q}_1 \tag{37a,b,c}$$

$$\mathbf{u}_2 = \mathbf{A}_2^0\mathbf{q}_2 + \mathbf{C}_0\hat{\mathbf{u}}_2 + \mathbf{C}_1'\,\hat{\mathbf{u}}_{2,x} + \mathbf{C}_2\hat{\mathbf{u}}_{2,xx} + \mathbf{C}_3\hat{\mathbf{u}}_{2,xxx} \tag{37d}$$

$$\mathbf{u}_{2,x} = \mathbf{A}_2^1\mathbf{q}_2 + \mathbf{C}_0\hat{\mathbf{u}}_{2,x} + \mathbf{C}_1'\,\hat{\mathbf{u}}_{2,xx} + \mathbf{C}_2\hat{\mathbf{u}}_{2,xxx} \tag{37e}$$

$$\mathbf{u}_{2,xx} = \mathbf{A}_2^2\mathbf{q}_2 + \mathbf{C}_0\hat{\mathbf{u}}_{2,xx} + \mathbf{C}_1'\,\hat{\mathbf{u}}_{2,xxx} \tag{37f}$$

$$\mathbf{u}_{2,xxx} = \mathbf{A}_2^3\mathbf{q}_2 + \mathbf{C}_0\hat{\mathbf{u}}_{2,xxx}, \quad \mathbf{u}_{2,xxx} = \mathbf{q}_2 \tag{37g,h}$$

where $\mathbf{A}_1^i, \mathbf{A}_2^j (i=0,1)$, $(j=0,1,2,3)$ are $L\times L$ known matrices; $\mathbf{C}_0$, $\mathbf{C}_1$, $\mathbf{C}_1'$, $\mathbf{C}_2$, $\mathbf{C}_3$ are $L\times 2$ known matrices and $\mathbf{u}_i$, $\mathbf{u}_{i,x}$, $\mathbf{u}_{i,xx}$, $\mathbf{u}_{i,xxx}$, $\mathbf{u}_{i,xxxx}$ are time dependent vectors including the values of $u_i(x,t)$ and their derivatives at the L nodal points. Eqs. (37a,b,d,e,f,g) can be assembled more conveniently as

$$\mathbf{u}_1 = \mathbf{H}_1^0\mathbf{d}_1, \quad \mathbf{u}_{1,x} = \mathbf{H}_1^1\mathbf{d}_1 \tag{38a,b}$$

$$\mathbf{u}_2 = \mathbf{H}_2^0\mathbf{d}_2, \quad \mathbf{u}_{2,x} = \mathbf{H}_2^1\mathbf{d}_2, \quad \mathbf{u}_{2,xx} = \mathbf{H}_2^2\mathbf{d}_2, \quad \mathbf{u}_{2,xxx} = \mathbf{H}_2^3\mathbf{d}_2 \tag{38c,d,e,f}$$

where $\mathbf{d}_1^{\mathrm{T}}=\{\mathbf{q}_1\ \ \hat{\mathbf{u}}_1\ \ \hat{\mathbf{u}}_{1,x}\}$, $\mathbf{d}_2^{\mathrm{T}}=\{\mathbf{q}_2\ \ \hat{\mathbf{u}}_2\ \ \hat{\mathbf{u}}_{2,x}\ \ \hat{\mathbf{u}}_{2,xx}\ \ \hat{\mathbf{u}}_{2,xxx}\}$ are generalized unknown vectors and $\mathbf{H}_1^i, \mathbf{H}_2^j$ $(i=0,1)$, $(j=0,1,2,3)$ are $L\times(L+4)$ and $L\times(L+8)$ known matrices, respectively, arising from $\mathbf{A}_1^i$, $\mathbf{A}_2^j$, $\mathbf{C}_0$, $\mathbf{C}_1$, $\mathbf{C}_1'$, $\mathbf{C}_2$, $\mathbf{C}_3$.

Applying Eqs. (17) to the L collocation points and employing Eqs. (38), $2L$ semidiscretized nonlinear equations of motion are formulated as

$$\mathbf{M}\begin{Bmatrix}\ddot{\mathbf{d}}_1\\ \ddot{\mathbf{d}}_2\end{Bmatrix}+\mathbf{K}\begin{Bmatrix}\mathbf{d}_1\\ \mathbf{d}_2\end{Bmatrix}+\mathbf{k}^{\mathrm{nl}}(\mathbf{H}_1^i,\mathbf{H}_2^j,\mathbf{d}_1,\mathbf{d}_2)=\mathbf{f} \tag{39}$$

where $\mathbf{k}^{\mathrm{nl}}$ is a nonlinear generalized stiffness vector and $\mathbf{M},\mathbf{K},\mathbf{f}$ are generalized mass matrix, stiffness matrix and force vector, respectively, given in Appendix B.

Eqs. (38a, c) when combined with Eqs. (18a, c) yield the following $2L$ linear equations with respect to $\mathbf{d}_1$, $\mathbf{d}_2$ for $t=0$

$$\mathbf{H}_1^0\mathbf{d}_1(0)=\overline{\mathbf{u}}_{\mathbf{m0}},\quad \mathbf{H}_2^0\mathbf{d}_2(0)=\overline{\boldsymbol{\theta}}_{\mathbf{0}} \tag{40a,b}$$

The above equations, together with Eqs. (35) written for $t=0$, form a set of $2L+12$ nonlinear algebraic equations which are solved to establish the initial conditions $\mathbf{d}_1(0)$, $\mathbf{d}_2(0)$. Similarly, Eqs. (38a, c) when combined with Eqs. (18b, d) yield the following $2L$ linear equations with respect to $\dot{\mathbf{d}}_1$, $\dot{\mathbf{d}}_2$ for $t=0$:

$$\mathbf{H}_1^0\dot{\mathbf{d}}_1(0)=\dot{\overline{\mathbf{u}}}_{\mathbf{m}0},\quad \mathbf{H}_2^0\dot{\mathbf{d}}_2(0)=\dot{\overline{\boldsymbol{\theta}}}_{\mathbf{0}} \tag{41a,b}$$

The above equations, together with 12 equations resulting after differentiating Eqs. (35) with respect to time and writing them for $t=0$, form a set of $2L+12$ linear algebraic equations, from which the initial conditions $\dot{\mathbf{d}}_1(0)$, $\dot{\mathbf{d}}_2(0)$ are established. It is worth here noting that in general, $\mathbf{d}_1(0)$, $\mathbf{d}_2(0)$ must be employed so that the system of equations can be resolved.

The aforementioned initial conditions along with Eqs. (35), (39) form an initial value problem of differential-algebraic equations (DAE) which can be solved using any efficient solver. In this study, the Petzold–Gear method is used [26] after introducing new variables to reduce the order of the system [27] and after differentiating Eqs. (35) with respect to time to obtain an equivalent system with a value of system index ind = 1 [26].

3.1.1. Reduced initial boundary value problem—free vibrations

The reduced initial boundary value problem described by Eqs. (26), (19b,c), (18c,d) can be similarly solved following the procedure presented above. Moreover, for the case of free vibrations, it can be assumed that points of reversal of motion exist, thus the following definitions are made [1,14]:

$$\dot{\theta}_{\max}=0,\quad \ddot{\theta}_{\max}=-\omega^2\cdot\theta_{\max} \tag{42a,b}$$

where the subscript max denotes the points at which reversal of motion occurs and ω^2 (here) denotes an eigenvalue-like quantity that is indicative of the intensity of the nonlinearity [14,28]. It is pointed out that ω does not correspond to the bar's natural frequency, since Eq. (26) apparently does not admit a variables separable solution, while for the same reason, the use of a single harmonic (as described in Eq. (42b)) leads to an approximate solution [29]. Substituting Eq. (42b) into Eq. (26) and taking into account that m_t, m_w along with β_3, $\overline{\beta}_3$ of Eqs. (26), (19b, c), respectively vanish, a nonlinear generalized eigenvalue problem is formulated as

$$[\mathbf{K}_r^{\mathrm{L}}+\mathbf{K}_r^{\mathrm{NL}}-\omega^2\mathbf{M}_r]\mathbf{d}_2=\mathbf{0} \tag{43}$$

where $\mathbf{K}_r^{\mathrm{NL}}$ is a nonlinear stiffness matrix and $\mathbf{M}_r,\mathbf{K}_r^{\mathrm{L}}$ are mass and stiffness matrices given in Appendix B.

The aforementioned problem is solved iteratively using the direct iteration technique (DIT) [14], following the algorithm presented in [1]. The algorithm is initiated with the fundamental mode shape $\mathbf{d}_2^f$ of the linear case (i.e. set $\mathbf{K}_r^{\mathrm{NL}}=\mathbf{0}$ in Eq. (43)) as a starting vector, while the normalization of the fundamental mode shape is performed by specifying the amplitude of the angle of twist $\overline{\theta}_{x0}$ at a selected cross-section.

The eigenvalue problem of Eq. (43) is indicative of the nonlinear behavior of the bar and does not provide solution in the time domain, while the arising eigenvalues and mode shapes depend on the amplitude of the initial conditions. For the case of axially immovable ends, $\tilde{N}$ is computed in each iteration by numerical integration of Eq. (24) after employing the aforementioned discretization of the bar, the constant element assumption and Eq. (38d). The computed eigenvalues are positive except 8 infinite ones which are ignored, since the mass matrix $\mathbf{M}_r$ (Eq. (B.2c)) contains 8 rows of zero elements.

3.2. For the primary warping function ϕ_S^P

The integral representations and the numerical solution for the evaluation of the axial displacement u_m and the angle of twist θ_x presented in the previous section assume that the warping C_S and the torsion I_t constants from Eqs. (11b,c) are already established. Eqs. (11b,c) indicate that the evaluation of the aforementioned constants presumes that the primary warping function ϕ_S^P at any interior point of the domain Ω of the cross-section of the bar is known. Once ϕ_S^P is established, C_S and I_t constants are evaluated by converting the domain integrals into line integrals along the boundary using the corresponding relations presented in Sapountzakis and Mokos [16].

Moreover, the evaluation of the primary warping function ϕ_S^P with respect to the shear center S and of its derivatives with respect to y and z at any interior point for the calculation of the stress components (Eqs. (4)) is accomplished using BEM [30] as this is presented in [31,32]. Finally, since the nonlinear torsional vibrations problem is solved by the BEM, the domain integrals of Eqs. (11a) and (16) have to be converted to boundary line ones, employing integration by parts, the Gauss theorem and the Green identity as

$$I_P = \frac{1}{3}\int_\Gamma (y^3 n_y + z^3 n_z)\,\mathrm{d}s \tag{44a}$$

$$I_{PP} = \int_\Gamma \left[\left(\frac{1}{5}y^5 + \frac{1}{3}y^3 z^2\right)n_y + \left(\frac{1}{5}z^5 + \frac{1}{3}y^2 z^3\right)n_z\right]\mathrm{d}s \tag{44b}$$

4. Numerical examples

On the basis of the analytical and numerical procedures presented in the previous sections, a computer program has been written and representative examples have been studied to demonstrate the efficiency, wherever possible the verification and the range of applications of the developed method. It is noted that the probability of the bar's exhibiting chaotic motion in its nonlinear response is not investigated within the present study. Moreover, the bar's material is assumed to be within the linear elastic range and the strains are considered to be small regardless of the magnitude of the bar's angle of twist θ_x. In all the examples treated, an I-shaped cross-section bar ($E = 2.1 \times 10^8\,\mathrm{kN\,m^{-2}}$, $G = 8.1 \times 10^7\,\mathrm{kN\,m^{-2}}$, $\rho = 8.002\,\mathrm{kN\,s^2\,m^{-4}}$) of length $l = 4.0\,\mathrm{m}$, having flange and web width $t_f = t_w = 0.01\,\mathrm{m}$, total height and total width $h = b = 0.20\,\mathrm{m}$ has been studied, while the numerical results have been obtained employing 21 nodal points (longitudinal discretization) and 400 boundary elements (cross-section discretization). The geometric constants of the bar are given in Table 1.

Example 1. In the first example, for comparison reasons, the free vibrations of the aforementioned bar with various boundary conditions have been studied. More specifically, the generalized eigenvalue problem of Eq. (43) (reduced initial boundary value problem) has been solved to obtain the dynamic characteristics at the points of reversal of motion. A member with simply supported torsional boundary conditions is firstly considered. In Table 2, the fundamental natural frequency ω^f and the induced axial load $\tilde{N}$ of the bar with simply supported torsional boundary conditions and axially immovable ends are presented for both the linear and three nonlinear cases with various initial midpoint angle of twist $\overline{\theta}_{x0}(l/2)$ amplitudes, taking into account all the nonlinear terms of Eqs. (26)–(27) ($I_n \neq 0$) or ignoring the geometric cross-sectional constant $I_n = 0$. In this table, the obtained results from the proposed method ignoring the aforementioned constant are compared with those obtained from a FEM solution [1], verifying the presented formulation (the discrepancy of the values is attributed to the inaccuracies of Vlasov's thin-walled beam theory employed by the authors in [1]). Moreover, the influence of the nonlinear terms related to the geometric cross-sectional constant I_n is remarked especially for large amplitudes of vibration.

In Table 3, the fundamental natural frequency ω^f of the bar with simply supported torsional boundary conditions subjected to a constant with respect to time axial load $\overline{N}(l,t)$ at its right end is presented for both the linear and three nonlinear cases with various initial midpoint angle of twist $\overline{\theta}_{x0}(l/2)$ amplitudes and for various values of this load (tensile, vanishing and two compressive ones), the last of which corresponds to a torsional post-buckled state, demonstrating the efficiency of the proposed formulation. It is worth here noting that in the post-buckling case the initial midpoint angle of twist amplitude cannot be arbitrary, since it must be greater than the one corresponding to the static (post-buckled) equilibrium state.

Moreover, in Tables 4 and 5 the same quantities with the respective ones of Tables 2 and 3 of the bar with a simply supported left end and a clamped right end as torsional boundary conditions are presented, while in Table 6 the obtained values of the fundamental mode shape of the angle of twist at selected points along the bar ignoring the geometric cross-sectional constant $I_n = 0$ are presented as compared with those obtained from a FEM solution [1] (case of axially immovable ends as axial boundary conditions). Once again, the verification and the efficiency of the proposed method are

Table 1
Geometric constants of the bar of the numerical examples.

$A\,(\mathrm{m^2})$	5.800×10^{-3}
$I_P\,(\mathrm{m^4})$	5.434×10^{-5}
$I_{PP}\,(\mathrm{m^6})$	6.722×10^{-7}
$I_n\,(\mathrm{m^6})$	1.631×10^{-7}
$I_t\,(\mathrm{m^4})$	2.080×10^{-7}
$C_S\,(\mathrm{m^6})$	1.200×10^{-7}

Table 2
Fundamental natural frequency ω^f and induced axial load $\tilde{N}$ of the bar of Example 1 with simply supported torsional boundary conditions and axially immovable ends.

	Present study		Rozmarynowski and Szymszak [1]
	$I_n \neq 0$	$I_n = 0$	$I_n = 0$
ω^f (s^{-1})			
Linear	214.23	214.23	207.23
$\overline{\theta}_{x0}(l/2) = 0.1$ rad	215.04	214.78	207.83
$\overline{\theta}_{x0}(l/2) = 0.2$ rad	217.44	216.40	209.62
$\overline{\theta}_{x0}(l/2) = 1.5$ rad	348.86	313.77	–
$\tilde{N}$(kN)			
Linear	–	–	–
$\overline{\theta}_{x0}(l/2) = 0.1$ rad	17.60 (3)	17.60 (3)	19.43
$\overline{\theta}_{x0}(l/2) = 0.2$ rad	70.36 (3)	70.39 (3)	77.72
$\overline{\theta}_{x0}(l/2) = 1.5$ rad	3891.26 (5)	3959.63 (3)	–

Values in parentheses indicate the performed iterations to obtain a numerical accuracy of order 10^{-6} to the convergence criterion.

Table 3
Fundamental natural frequency ω^f of the bar of Example 1 with simply supported torsional boundary conditions and constant axial load.

	$\overline{N}(l,t)$(kN)			
	1000	0	−1000	−4000
Linear	243.25	214.23	180.62	–
$\overline{\theta}_{x0}(l/2) = 0.1$ rad	243.48 (2)	214.49 (2)	180.93 (2)	–[a]
$\overline{\theta}_{x0}(l/2) = 0.2$ rad	244.17 (3)	215.28 (3)	181.86 (3)	–[a]
$\overline{\theta}_{x0}(l/2) = 1.5$ rad	288.46 (5)	264.36 (5)	237.82 (5)	128.61 (6)

Values in parentheses indicate the performed iterations to obtain a numerical accuracy of order 10^{-6} to the convergence criterion.
[a] Equilibrium cannot be reached.

Table 4
Fundamental natural frequency ω^f and induced axial load $\tilde{N}$ of the bar of Example 1 with simply supported left end, clamped right end as torsional boundary conditions and axially immovable ends.

	Present study		Rozmarynowski and Szymszak [1]
	$I_n \neq 0$	$I_n = 0$	$I_n = 0$
ω^f (s^{-1})			
Linear	285.21	285.21	279.53
$\overline{\theta}_{x0}(l/2) = 0.1$ rad	285.99	285.73	280.09
$\overline{\theta}_{x0}(l/2) = 0.2$ rad	288.32	287.26	281.77
$\overline{\theta}_{x0}(l/2) = 1.5$ rad	414.66	379.93	–
$\tilde{N}$(kN)			
Linear	–	–	–
$\overline{\theta}_{x0}(l/2) = 0.1$ rad	19.21 (3)	19.22 (3)	21.27
$\overline{\theta}_{x0}(l/2) = 0.2$ rad	76.73 (4)	76.82 (3)	85.03
$\overline{\theta}_{x0}(l/2) = 1.5$ rad	4067.54 (6)	4190.79 (6)	–

Values in parentheses indicate the performed iterations to obtain a numerical accuracy of order 10^{-6} to the convergence criterion.

illustrated. Noting the aforementioned Tables 2–6, it is easily verified that the geometrical nonlinearity alters the mode shapes of vibration, induces a stiffening axial force in the case of axially immovable ends and stiffens the structure leading to higher natural frequencies, which are the main aspects of the nonlinear torsional free vibration analysis. Obviously these effects are more pronounced with the increase of the initial midpoint angle of twist amplitude.

Table 5
Fundamental natural frequency ω^f of the bar of Example 1 with simply supported left end, clamped right end as torsional boundary conditions and constant axial load.

	$\overline{N}(l,t)$(kN)			
	1000	0	−1000	−5230
Linear	310.68	285.21	257.01	–
$\overline{\theta}_{x0}(l/2)=0.1$ rad	310.92 (2)	285.48 (2)	257.32 (2)	–[a]
$\overline{\theta}_{x0}(l/2)=0.2$ rad	311.64 (3)	286.29 (3)	258.23 (3)	14.35 (4)
$\overline{\theta}_{x0}(l/2)=1.5$ rad	356.30 (5)	334.97 (6)	312.12 (6)	185.58 (7)

Values in parentheses indicate the performed iterations to obtain a numerical accuracy of order 10^{-6} to the convergence criterion.
[a] Equilibrium cannot be reached.

Table 6
Fundamental mode shape of the angle of twist at points along the bar of Example 1 with simply supported left end, clamped right end as torsional boundary conditions and axially immovable ends.

x/l	$\overline{\theta}_{x0}(l/2)$(rad)							
	Linear		0.1		0.2		1.5	
	Present study ($I_n=0$)	Rozmarynowski and Szymszak [1] Rozmarynowski and Szymszak [1]	Present study ($I_n=0$)	Rozmarynowski and Szymszak [1]	Present study ($I_n=0$)	Rozmarynowski and Szymszak [1]	Present study ($I_n=0$)	
0	0	0	0	0	0	0	0	–
0.125	0.4629	0.4645	0.4627	0.4643	0.4624	0.4640	0.44440	–
0.25	0.8270	0.8295	0.8268	0.8294	0.8263	0.8288	0.8000	–
0.375	1.0171	1.0192	1.0169	1.0191	1.0166	1.0187	0.9971	–
0.5	1	1	1	1	1	1	1	–
0.625	0.7925	0.7912	0.7926	0.7913	0.7930	0.7917	0.8151	–
0.75	0.4689	0.4665	0.4691	0.4667	0.4696	0.4673	0.5013	–
0.875	0.1501	0.1485	0.1502	0.1486	0.1505	0.1490	0.1691	–
1	0	0	0	0	0	0	0	–

Example 2. In the second example, the free vibrations of the simply supported bar (according to the torsional boundary conditions) with various initial conditions has been studied. Both the complete and the reduced initial boundary value problems presented in the previous sections have been solved to obtain the response of the bar in the time domain. The linear fundamental mode shape of the angle of twist is firstly considered as initial twisting rotations $\overline{\theta}_{x0}(x)$ along with zero initial twisting velocities $\dot{\overline{\theta}}_{x0}(x)$, to the beam with immovable left and free right end according to the axial boundary conditions. The normalization of the mode shape is performed by specifying the amplitude of the angle of twist at the midpoint of the bar.

In Figs. 3 and 4 the time histories of characteristic kinematical components (angle of twist $\theta_x(l/2,t)$ at the midpoint of the bar, axial displacement $u_m(l,t)$ at the bar's right end) and the twisting moment at the bar's left end $M_t(0,t)$, respectively, are presented for two values of the initial midpoint angle of twist amplitude ($\overline{\theta}_{x0}(l/2)=1.5$ rad, $\overline{\theta}_{x0}(l/2)=0.2$ rad) performing two cases of analysis, namely a linear one employing the proposed method and ignoring the nonlinear terms of Eqs. (17), (20) and a nonlinear—reduced initial boundary value problem of Eqs. (26), (18c,d), (19b,c). From these figures, the effects of both the nonlinear terms and the initial midpoint angle of twist amplitude are observed on both the kinematical and stress components. Moreover, from Fig. 3a, the natural frequency of the angle of twist $\theta_x(l/2,t)$ (nonlinear analysis case, $\overline{\theta}_{x0}(l/2)=1.5$ rad) is computed as $\omega^f=255.41\,\mathrm{s}^{-1}$, thus exhibiting a variation of 3.4 percent as compared with the corresponding value of the frequency-like quantity presented in Table 3 ($\omega^f=264.36\,\mathrm{s}^{-1}$). Thus, as it is already mentioned, the frequency-like values obtained from the solution of the eigenvalue problem of Eq. (43) should not be confused with the actual natural frequencies of the bar. It is worth here noting that the pronounced alteration of the twisting moment's time history pattern and a slight change of the amplitude of the angle of twist (which is not clearly shown in Fig. 3a) are attributed to the fact that the fundamental nonlinear mode shape does not coincide with the linear one. Moreover, as it is easily verified from Fig. 3, the frequency of the axial displacement's response is twice as much as the one of the twisting rotation's one.

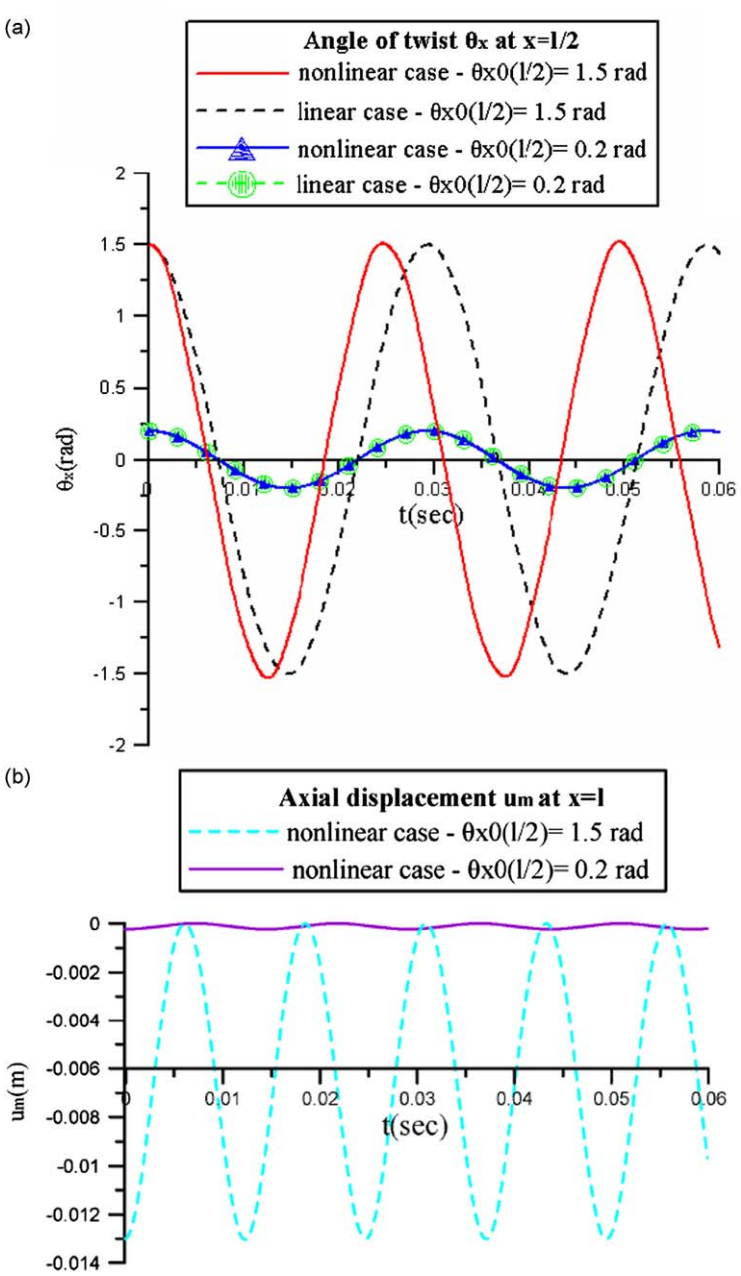

Fig. 3. Time histories of the angle of twist at the midpoint (a) and axial displacement at the right end point (b) of the bar of Example 2, for the case of initial twisting rotations $\overline{\theta}_{x0}(x)$.

Moreover, the case of constant along the bar initial twisting velocities $\dot{\overline{\theta}}_{x0}(x) = 50\,\mathrm{rad\,s^{-1}}$, variable along the bar initial axial displacements given from $\overline{u}_{m0}(x) = [\overline{N}(l,0)/(EA)]x$, along with vanishing initial twisting rotations $\overline{\theta}_{x0}(x) = 0$ and initial axial velocities $\dot{\overline{u}}_{m0}(x) = 0$, applied to the bar with immovable left and free right end subjected to constant axial load $\overline{N}(l,t) = -3000\,\mathrm{kN}$ according to the axial boundary conditions, has been also studied. In Fig. 5 the time history of the angle of twist $\theta_x(l/2,t)$ at the midpoint of the bar is presented for three cases of analysis, namely a linear one, a nonlinear-complete and a reduced initial boundary value problem, as these were presented in the previous sections. The main conclusions of the nonlinear torsional free vibration analysis are once again verified. In Fig. 6, the time histories of the axial stress resultant at the bar's left end $N(0,t)$ and of the axial displacement at the bar's right end $u_m(l,t)$ are presented for three cases of analysis. Apparently, the time dependent response of the axial stress resultant can only be estimated by solving the

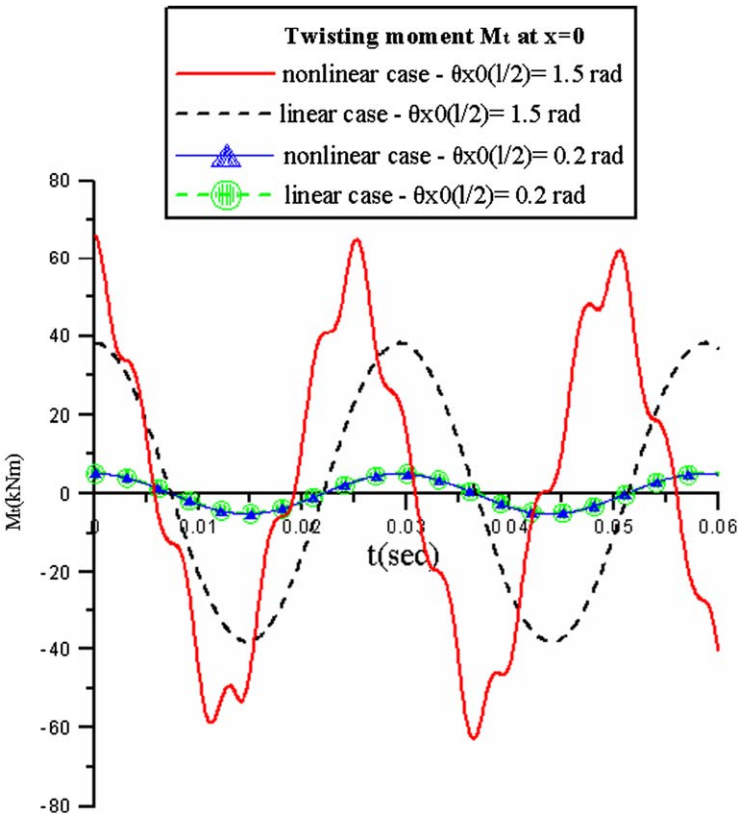

Fig. 4. Time history of the twisting moment at the left end of the bar of Example 2, for the case of initial twisting rotations $\overline{\theta}_{x0}(x)$.

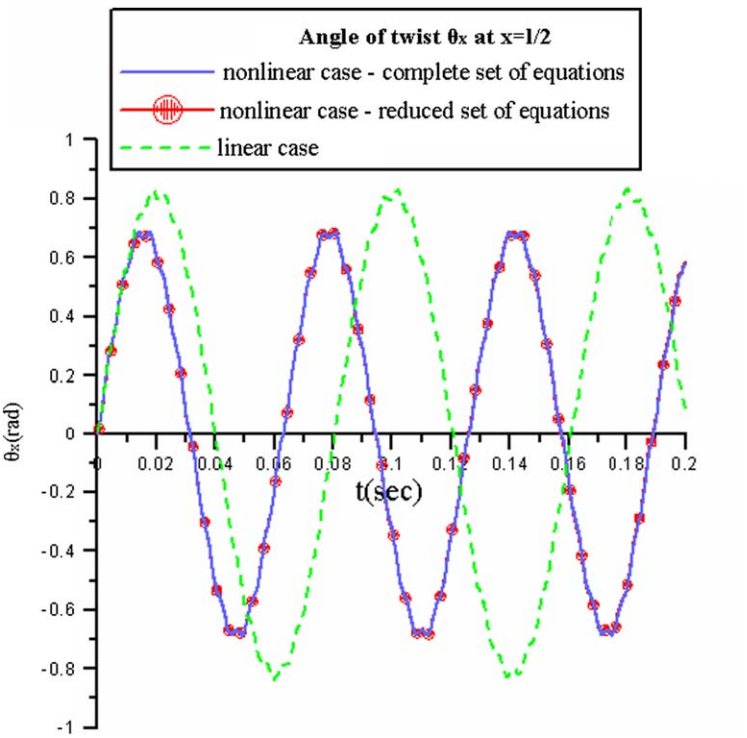

Fig. 5. Time history of the angle of twist at the midpoint of the bar of Example 2, for the case of initial twisting velocities $\dot{\overline{\theta}}_{x0}(x)$ and initial axial displacements $\overline{u}_{m0}(x)$.

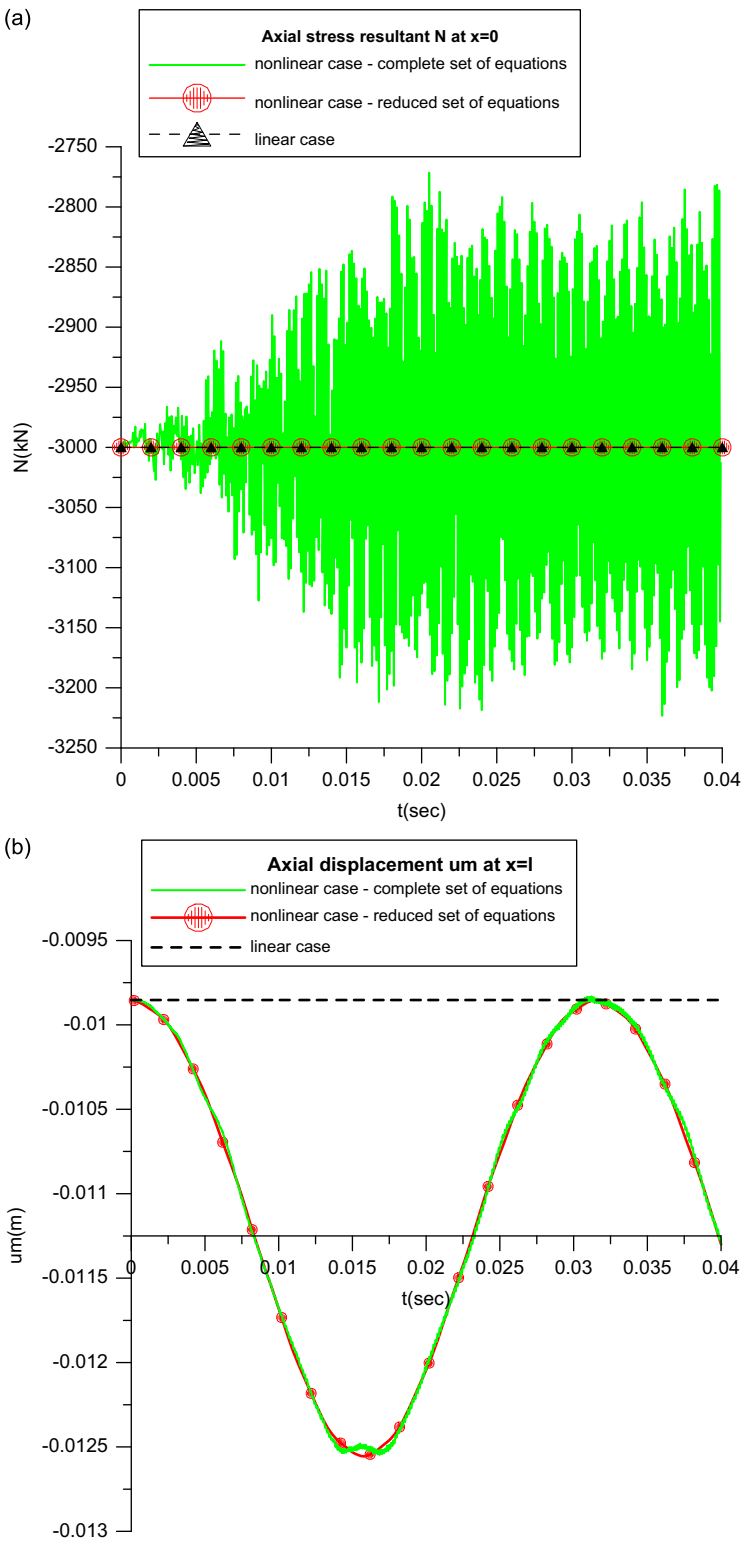

Fig. 6. Time histories of the axial stress resultant at the left end (a) and the axial displacement at the right end (b) of the bar of Example 2, for the case of initial twisting velocities $\overline{\dot{\theta}}_{x0}(x)$ and initial axial displacements $\overline{u}_{m0}(x)$.

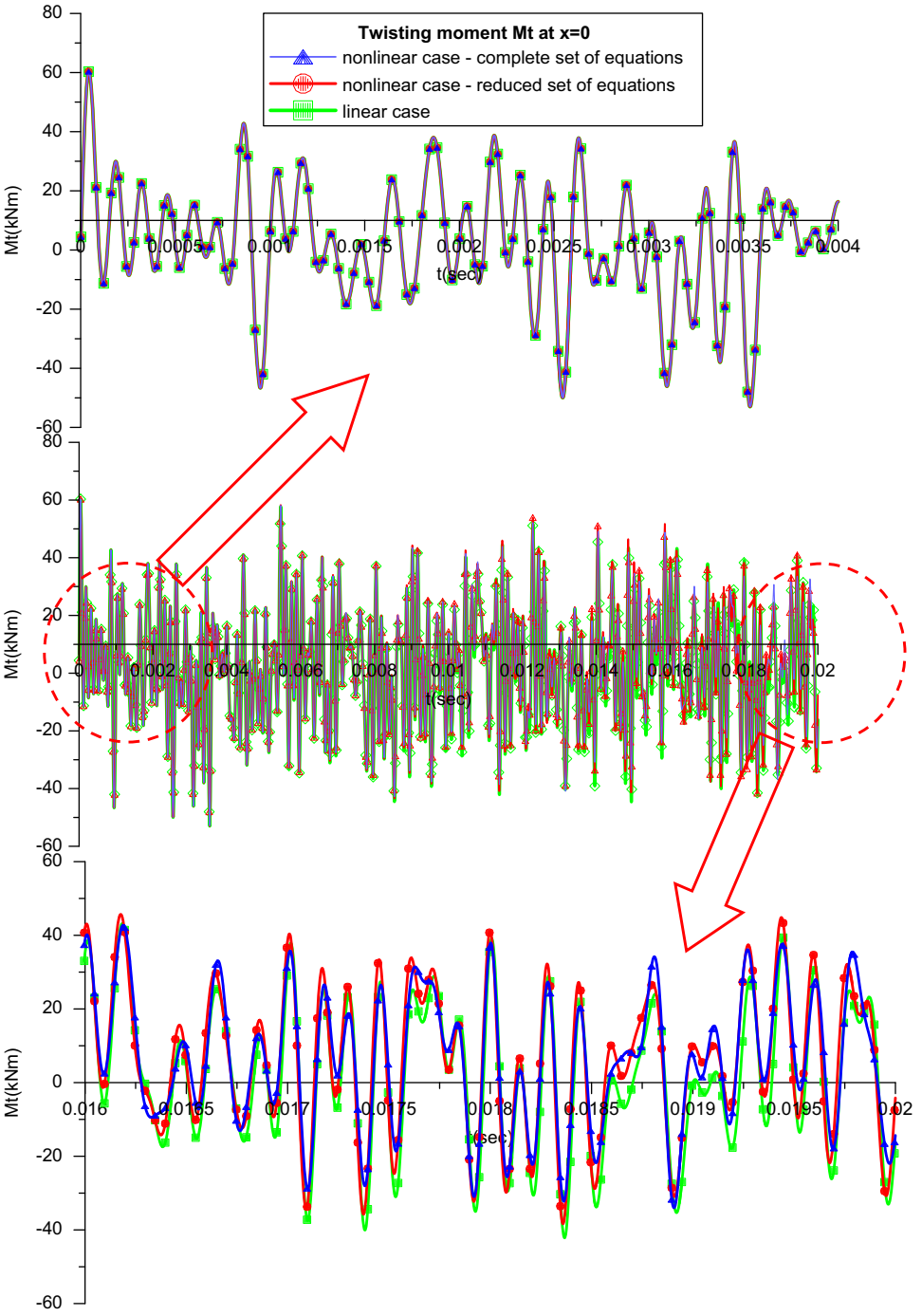

Fig. 7. Time history of the twisting moment at the left end of the bar of Example 2, for the case of initial twisting velocities $\dot{\overline{\theta}}_{x0}(x)$ and initial axial displacements $\overline{u}_{m0}(x)$.

complete initial boundary value problem, while the discrepancy of its extreme values compared with the initial one is remarkable. Thus, the influence of the axial inertia term $\rho A \cdot \ddot{u}_m$ on the axial stress resultant is pointed out, while from Figs. 5 and 6b its influence on the kinematical components is proved to be negligible. Moreover, it is once again observed that the frequency of the axial displacement's response is twice as much as the one of the twisting rotation's one. Finally, in Fig. 7, the time history of the twisting moment $M_t(0,t)$ at the bar's left end for the aforementioned cases of analysis are

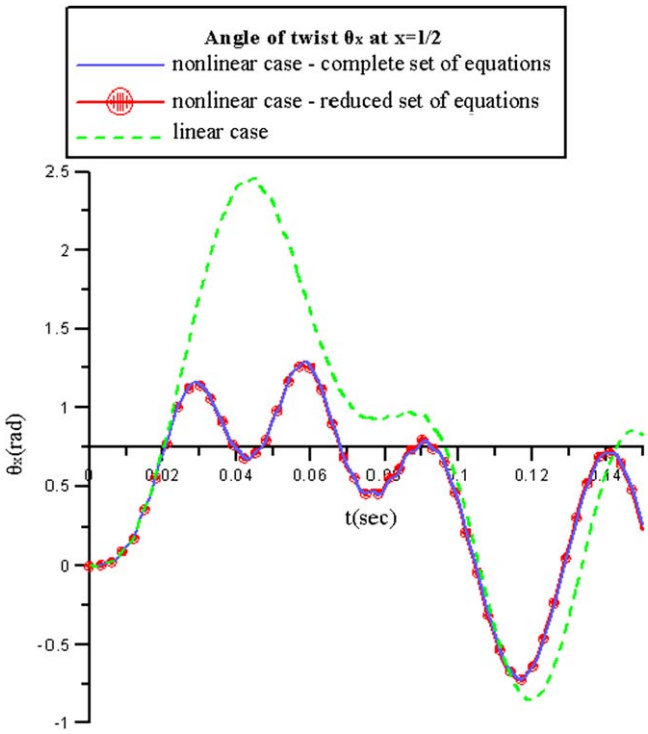

Fig. 8. Time history of the angle of twist at the midpoint of the bar of Example 3.

presented demonstrating the time dependent influence of the axial inertia term $\rho A \cdot \ddot{u}_m$ on the aforementioned stress resultant.

Example 3. In order to demonstrate the range of applications of the developed method, in the third example the forced vibrations of the simply supported bar (according to the torsional boundary conditions) subjected to a moving concentrated twisting moment has been studied. All of the initial conditions are zero except from the initial axial displacements, which are given from $\overline{u}_{m0}(x) = [\overline{N}(l,0)/(EA)]x$, while the bar has an immovable left and free right end subjected to constant axial load $\overline{N}(l,t) = -2500\,\text{kN}$ according to the axial boundary conditions. The concentrated twisting moment has a constant numerical value $M_t = 20.0\,\text{kN m}$ and "travels" with a constant velocity $\upsilon = 40\,\text{m s}^{-1}$, thus the bar is subjected to free vibrations after $t = 0.1$ s. In Fig. 8 the time history of the angle of twist $\theta_x(l/2,t)$ at the midpoint of the bar is presented for the aforementioned cases of analysis (linear, nonlinear-complete and reduced initial boundary value problems) demonstrating the discrepancy of the nonlinear response of the bar compared with that of the linear one in both its forced and free vibrating phase. In Fig. 9, the time histories of the axial stress resultant at the bar's left end $N(0,t)$ and of the axial displacement at the bar's right end $u_m(l,t)$ are presented for three cases of analysis. The conclusions already drawn from Example 2 are verified. Finally, in Table 7 the extreme values of characteristic kinematical components and the axial stress resultant $N(0,t)$ at the bar's left end, computed in the time domain $0.0 \le t \le 0.15$ (s) are presented, demonstrating the influence of the geometrical nonlinearity and the axial inertia term $\rho A \cdot \ddot{u}_m$ on them.

5. Concluding remarks

In this paper a boundary element method is developed for the nonuniform torsional vibration problem of simply or multiply connected cylindrical bars of arbitrary doubly symmetric cross-section, taking into account the effect of geometrical nonlinearity. The main conclusions that can be drawn from this investigation are

(a) The numerical technique presented in this investigation is well suited for computer aided analysis of cylindrical bars of arbitrarily shaped doubly symmetric cross-section, supported by the most general boundary conditions and subjected to the combined action of arbitrarily distributed or concentrated time dependent conservative axial and torsional loading.
(b) The geometrical nonlinearity leads to coupling between the torsional and axial equilibrium equations. Moreover, the arising nonlinear terms alter the mode shapes of vibration.

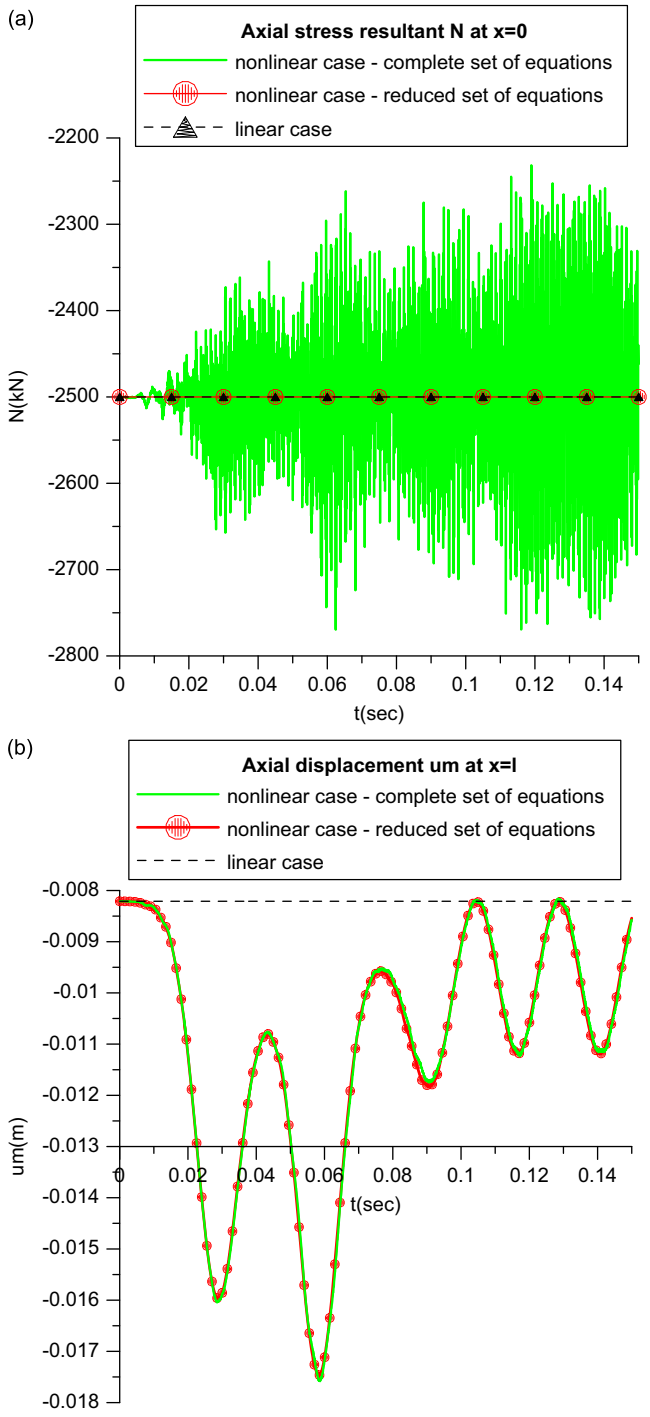

Fig. 9. Time histories of the axial stress resultant at the left end (a) and the axial displacement at the right end (b) of the bar of Example 3.

(c) Large twisting rotations increase the torsional stiffness of the bar, leading eventually to higher natural frequencies. Moreover, a tensile axial force is induced in the bar for special cases of axial boundary conditions resulting also in the aforementioned effects.

(d) In the treated examples, the axial inertia term $\rho A \cdot \ddot{u}_m$ affects the stress resultants (especially the axial one), while its influence proves to be negligible on the kinematical components.

(e) The developed procedure retains most of the advantages of a BEM solution over a FEM approach, although it requires longitudinal domain discretization.

Table 7
Extreme values of various kinematical components and stress resultants at the time domain $0.0 \le t \le 0.15$ s of the bar of Example 3.

	Linear	Nonlinear-reduced set of equations	Nonlinear-complete set of equations
$\max \theta_x(l/2,t)$ (rad)	2.456	1.290	1.290
$\min \theta_x(l/2,t)$ (rad)	-8.549×10^{-1}	-7.294×10^{-1}	-7.244×10^{-1}
$\max \theta'_x(0,t)$ (rad m^{-1})	1.970	9.818×10^{-1}	9.829×10^{-1}
$\min \theta'_x(0,t)$ (rad m^{-1})	-6.844×10^{-1}	-5.688×10^{-1}	-5.645×10^{-1}
$\max \theta''_x(l/2,t)$ (rad m^{-2})	6.315×10^{-1}	5.696×10^{-1}	5.304×10^{-1}
$\min \theta''_x(l/2,t)$ (rad m^{-2})	-1.721	$-9.19-10^{-1}$	-1.000
$\max u_m(l,t)$ (m)	-8.210×10^{-3}	-8.210×10^{-3}	-8.159×10^{-3}
$\min u_m(l,t)$ (m)	-8.210×10^{-3}	-1.746×10^{-2}	-1.758×10^{-2}
$\max u'_m(l,t)$ (m m^{-1})	-2.053×10^{-3}	-2.053×10^{-3}	-2.053×10^{-3}
$\min u'_m(l,t)$ (m m^{-1})	-2.053×10^{-3}	-6.725×10^{-3}	-6.718×10^{-3}
$\max N(0,t)$ (kN)	-2.500×10^{3}	-2.500×10^{3}	-2.798×10^{3}
$\min N(0,t)$ (kN)	-2.500×10^{3}	-2.500×10^{3}	-2.200×10^{3}

Acknowledgments

The authors would like to thank the Senator Committee of Basic Research of the National Technical University of Athens, Programme "PEVE-2008", R.C. no: 65 for the financial support of this work.

Appendix A

Kernels $\Lambda_j(r)$, $(j=1,2,3,4)$ ($r=x-\xi$, x, ξ points of the bar) appearing in the integral representations of the numerical solution (Section 3):

$$\Lambda_1(r) = -\frac{1}{2}\operatorname{sgn}\frac{r}{l}, \quad \Lambda_2(r) = -\frac{1}{2}l\left(1-\left|\frac{r}{l}\right|\right) \tag{A.1a,b}$$

$$\Lambda_3(r) = -\frac{1}{4}l^2\left|\frac{r}{l}\right|\left(\left|\frac{r}{l}\right|-2\right)\operatorname{sgn}\frac{r}{l}, \quad \Lambda_4(r) = \frac{1}{12}l^3\left(2+\left|\frac{r}{l}\right|^3-3\left|\frac{r}{l}\right|^2\right) \tag{A.2c,d}$$

Appendix B

Generalized mass matrix $\mathbf{M}$, stiffness matrix $\mathbf{K}$, force vector $\mathbf{f}$ and nonlinear generalized stiffness vector $\mathbf{k}^{\mathrm{nl}}$ arising from the initial value problem of Section 3:

$$\mathbf{M} = \begin{bmatrix} \rho A\cdot\mathbf{H}_1^0 & \mathbf{0} \\ \mathbf{0} & \rho I_P\cdot\mathbf{H}_2^0-\rho C_S\cdot\mathbf{H}_2^2 \end{bmatrix} \tag{B.1a}$$

$$\mathbf{K} = \begin{bmatrix} -EA\cdot\mathbf{I0}_1 & \mathbf{0} \\ \mathbf{0} & -GI_t\cdot\mathbf{H}_2^2+EC_S\cdot\mathbf{I0}_2 \end{bmatrix} \tag{B.1b}$$

$$\mathbf{f} = \begin{Bmatrix} \mathbf{n} \\ \mathbf{m}_t+\mathbf{m}'_w \end{Bmatrix} \tag{B.1c}$$

$$(\mathbf{k}^{\mathrm{nl}})_i = -EI_P((\mathbf{H}_2^1)_i\mathbf{d}_2)((\mathbf{H}_2^2)_i\mathbf{d}_2) \tag{B.1d}$$

$$(\mathbf{k}^{\mathrm{nl}})_{L+i} = -\tfrac{3}{2}EI_{PP}[(\mathbf{H}_2^1)_i\mathbf{d}_2]^2((\mathbf{H}_2^2)_i\mathbf{d}_2)-EI_P((\mathbf{H}_1^1)_i\mathbf{d}_1)((\mathbf{H}_2^2)_i\mathbf{d}_2)-EI_P(\mathbf{d}_1)_i((\mathbf{H}_2^1)_i\mathbf{d}_2) \tag{B.1e}$$

In Eqs. (B.1), $(\cdot)_i$ denotes the (arbitrary) i-th row ($i=1,2,\ldots,L$) of the matrix inside the brackets, $\mathbf{I0}_1=[\mathbf{I}\ \mathbf{0}_1]$, $\mathbf{I0}_2=[\mathbf{I}\ \mathbf{0}_2]$ are $L\times(L+4)$, $L\times(L+8)$ rectangular matrices, respectively, with $\mathbf{I}$, $\mathbf{0}_1$ and $\mathbf{0}_2$ being the $L\times L$ identity matrix, the $L\times4$ and the $L\times8$ rectangular matrices with zero elements, respectively, while $\mathbf{n},\mathbf{m}_t,\mathbf{m}'_w$ are vectors containing the values of the dynamic external loading at the L nodal points (the elements of $\mathbf{m}'_w$ are written with respect to the values of $m_w(x,t)$ at the corresponding collocation points after employing appropriate finite differences [33]).

Generalized nonlinear and linear stiffness matrices $\mathbf{K}_r^{\mathrm{NL}}, \mathbf{K}_r^{\mathrm{L}}$ and generalized mass matrix $\mathbf{M}_r$ arising from the eigenvalue problem of Section 3:

$$\mathbf{K}_r^{\mathrm{NL}} = \begin{cases} \begin{bmatrix} -\dfrac{I_P}{A}\tilde{N}(\mathbf{H}_2^2)_1 - \dfrac{3}{2}EI_n[(\mathbf{H}_2^1)_1\mathbf{d}_2]^2(\mathbf{H}_2^2)_1 \\ -\dfrac{I_P}{A}\tilde{N}(\mathbf{H}_2^2)_2 - \dfrac{3}{2}EI_n[(\mathbf{H}_2^1)_2\mathbf{d}_2]^2(\mathbf{H}_2^2)_2 \\ \vdots \\ -\dfrac{I_P}{A}\tilde{N}(\mathbf{H}_2^2)_L - \dfrac{3}{2}EI_n[(\mathbf{H}_2^1)_L\mathbf{d}_2]^2(\mathbf{H}_2^2)_L \end{bmatrix}, & \text{rows } 1,2,...,L \\ \begin{bmatrix} \mathbf{0} & \mathbf{0} & \mathbf{0} & \mathbf{0} & \mathbf{0} \\ \mathbf{0} & \mathbf{0} & \mathbf{0} & \mathbf{0} & \mathbf{0} \\ \mathbf{0} & \mathbf{0} & \dfrac{I_P}{A}\tilde{N}\cdot\mathbf{D}_{r1}^{\mathrm{nl}} + \dfrac{1}{2}EI_n\cdot\mathbf{D}_{r2}^{\mathrm{nl}}(\hat{\mathbf{u}}_2^2) & \mathbf{0} & \mathbf{0} \\ \mathbf{0} & \mathbf{0} & \mathbf{0} & \mathbf{0} & \mathbf{0} \end{bmatrix}, & \text{rows } L+1, L+2, ..., L+8 \end{cases} \tag{B.2a}$$

$$\mathbf{K}_r^{L} = \begin{cases} -GI_t\cdot\mathbf{H}_2^2 + EC_S\cdot I\mathbf{0} & \text{rows } 1,2,\ldots,L \\ \begin{bmatrix} \mathbf{F}_3 & \mathbf{E}_{35} & \mathbf{E}_{36} & \mathbf{E}_{37} & \mathbf{E}_{38} \\ \mathbf{F}_4 & \mathbf{0} & \mathbf{E}_{46} & \mathbf{E}_{47} & \mathbf{E}_{48} \\ \mathbf{0} & \mathbf{D}_{55} & \mathbf{D}_{56} & \mathbf{0} & \mathbf{D}_{58} \\ \mathbf{0} & \mathbf{0} & \mathbf{D}_{66} & \mathbf{D}_{67} & \mathbf{0} \end{bmatrix} & \text{rows } L+1, L+2, \ldots, L+8 \end{cases} \tag{B.2b}$$

$$\mathbf{M}_r = \begin{cases} \rho I_P\cdot\mathbf{H}_2^0\text{-}\rho C_S\cdot\mathbf{H}_2^2 & \text{rows } 1,2,\ldots,L \\ \mathbf{0} & \text{rows } L+1,\ L+2,\ldots,L+8 \end{cases} \tag{B.2c}$$

where $\mathbf{K}_r^{\mathrm{NL}}, \mathbf{K}_r^{\mathrm{L}}, \mathbf{M}_r$ are $(L+8)\times(L+8)$ square matrices, while $\mathbf{D}_{r1}^{\mathrm{nl}}$, $\mathbf{D}_{r2}^{\mathrm{nl}}(\hat{\mathbf{u}}_2^2)$ in Eq. (B.2a) are 2×2 rectangular ones including the values of the functions β_j $(j=1,2)$.

References

[1] B. Rozmarynowski, C. Szymczak, Non-linear free torsional vibrations of thin-walled beams with bisymmetric cross-section, *Journal of Sound and Vibration* 97 (1984) 145–152.
[2] M.R.M. Crespo Da Silva, Non-linear flexural-flexural-torsional-extensional dynamics of beams—I. formulation, *International Journal of Solids and Structures* 24 (1988) 1225–1234.
[3] M.R.M. Crespo Da Silva, Non-linear flexural-flexural-torsional-extensional dynamics of beams—II. Response analysis, *International Journal of Solids and Structures* 24 (1988) 1235–1242.
[4] P.F. Pai, A.H. Nayfeh, Three-dimensional nonlinear vibrations of composite beams—I. Equations of motion, *Nonlinear Dynamics* 1 (1990) 477–502.
[5] P.F. Pai, A.H. Nayfeh, Three-dimensional nonlinear vibrations of composite beams—II. Flapwise excitations, *Nonlinear Dynamics* 2 (1991) 1–34.
[6] P.F. Pai, A.H. Nayfeh, Three-dimensional nonlinear vibrations of composite beams—III. Chordwise excitations, *Nonlinear Dynamics* 2 (1991) 137–156.
[7] A. Di Egidio, A. Luongo, F. Vestroni, A non-linear model for the dynamics of open cross-section thin-walled beams—Part I: formulation, *International Journal of Non-Linear Mechanics* 38 (2003) 1067–1081.
[8] A. Di Egidio, A. Luongo, F. Vestroni, A non-linear model for the dynamics of open cross-section thin-walled beams—Part II: forced motion, *International Journal of Non-Linear Mechanics* 38 (2003) 1083–1094.
[9] J.C. Simo, L. Vu-Quoc, A Geometrically-exact rod model incorporating shear and torsion-warping deformation, *International Journal of Solids and Structures* 27 (1991) 371–393.
[10] P.F. Pai, A.H. Nayfeh, A fully nonlinear theory of curved and twisted composite rotor blades accounting for warpings and three-dimensional stress effects, *International Journal of Solids and Structures* 31 (1994) 1309–1340.
[11] F. Mohri, L. Azrar, M. Potier-Ferry, Vibration analysis of buckled thin-walled beams with open sections, *Journal of Sound and Vibration* 275 (2004) 434–446.
[12] S.P. Machado, V.H. Cortinez, Free vibration of thin-walled composite beams with static initial stresses and deformations, *Engineering Structures* 29 (2007) 372–382.
[13] J.T. Katsikadelis, The analog equation method. A boundary-only integral equation method for nonlinear static and dynamic problems in general bodies, *Theoretical and Applied Mechanics* 27 (2002) 13–38.
[14] G.R. Bhashyam, G. Prathap, Galerkin finite element method for non-linear beam vibrations, *Journal of Sound and Vibration* 72 (1980) 191–203.
[15] G. Chen, N.S. Trahair, Inelastic nonuniform torsion of steel I-beams, *Journal of Constructional Steel Research* 23 (1992) 189–207.
[16] E.J. Sapountzakis, V.G. Mokos, Warping shear stresses in nonuniform torsion by BEM, *Computational Mechanics* 30 (2003) 131–142.
[17] E. Ramm, T.J. Hofmann, Stabtragwerke, Der Ingenieurbau, in: G. Mehlhorn (Ed.), *Band Baustatik/Baudynamik*, Ernst & Sohn, Berlin, 1995.
[18] H. Rothert, V. Gensichen, *Nichtlineare Stabstatik*, Springer, Berlin, 1987.
[19] D.O. Brush, B.O. Almroth, *Buckling of Bars, Plates and Shells*, McGraw-Hill, New York, 1975.
[20] N.S. Trahair, Nonlinear elastic nonuniform torsion, *Journal of Structural Engineering* 131 (2005) 1135–1142.
[21] V. Vlasov, *Thin-Walled Elastic Beams*, Israel Program for Scientific Translations, Jerusalem, 1963.
[22] A.E. Armenakas, *Advanced Mechanics of Materials and Applied Elasticity*, Taylor & Francis, New York, 2006.
[23] S.P. Timoshenko, J.N. Goodier, *Theory of Elasticity*, McGraw-Hill, New York, 1970.
[24] V.G. Mokos, Contribution to the Generalized Theory of Composite Beams Structures by the Boundary Element Method, Ph.D. Thesis, National Technical University of Athens (in Greek), 2007.
[25] E.J. Sapountzakis, J.T. Katsikadelis, Elastic deformation of ribbed plate systems under static, transverse and inplane loading, *Computers and Structures* 74 (2000) 571–581.
[26] K.E. Brenan, S.L. Campbell, L.R. Petzold, *Numerical Solution of Initial-value Problems in Differential-Algebraic Equations*, North-Holland, Amsterdam, 1989.

[27] Z.P. Bazant, L. Cedolin, *Stability of Structures: Elastic, Inelastic, Fracture and Damage Theories*, Oxford University Press, New York, 1991.
[28] G. Prathap, T.K. Varadan, The large amplitude vibration of hinged beams, *Computers and Structures* 9 (1978) 219–222.
[29] R. Lewandowski, Nonlinear free-vibrations of beams by the finite-element and continuation methods, *Journal of Sound and Vibration* 170 (1994) 577–593.
[30] J.T. Katsikadelis, *Boundary Elements: Theory and Applications*, Elsevier, Amsterdam, London, 2002.
[31] E.J. Sapountzakis, Solution of nonuniform torsion of bars by an integral equation method, *Computers and Structures* 77 (2000) 659–667.
[32] E.J. Sapountzakis, V.G. Mokos, Nonuniform torsion of composite bars by boundary element method, *Journal of Engineering Mechanics, ASCE* 127 (9) (2001) 945–953.
[33] E.J. Sapountzakis, V.G. Mokos, Nonuniform torsion of bars of variable cross section, *Computers and Structures* 82 (2004) 703–715.